



## Contrasting Neogene–Quaternary continental margin evolution offshore mid-north Norway: Implications for source-to-sink systems

Stine Bjordal-Olsen<sup>a,\*</sup>, Tom Arne Rydningen<sup>a</sup>, Jan Sverre Laberg<sup>a</sup>, Amando P.E. Lasabuda<sup>a,b</sup>, Stig-Morten Knutsen<sup>c</sup>

<sup>a</sup> Department of Geosciences, UiT The Arctic University of Norway, N-9037 Tromsø, Norway

<sup>b</sup> Department of Earth Sciences, Royal Holloway University of London, Egham, UK

<sup>c</sup> The Norwegian Petroleum Directorate, Storgata 49, Harstad, Norway

### ARTICLE INFO

Editor: Michele Rebesco

#### Keywords:

Alongslope and downslope processes  
Source-to-sink  
Norwegian continental margin  
Cenozoic stratigraphy  
Hinterland and margin morphology  
Contourite drift

### ABSTRACT

The Neogene–Quaternary development of the ~700 km long mid-Norwegian and Lofoten–Vesterålen continental margin is reconstructed using a dense grid of 2D seismic data and exploration wellbores. Overall, widespread ocean current-controlled contourite drifts built up along the whole margin segment from the mid-Miocene onwards (c. 11 Ma, Kai Formation). The onset (c. 8.8 Ma) of a large inner shelf progradation (Molo Formation) was, however, restricted to the southern part of the study area, the inner mid-Norwegian shelf. In the Quaternary (c. 2.7 Ma), grounded ice sheets repeatedly brought large sediment volumes (Naust Formation) to the shelf beyond the Molo Formation. A similar build-out is less pronounced further north, where contourite drift growth instead continued and resulted in build-up of the Lofoten and Vesterålen drifts. In contrast, the drifts of the southern part of the study area occur for the most part stratigraphically below, interbedded with and distal to the progradational Molo and Naust deposits.

The study area exemplifies pronounced variability in Neogene–Quaternary continental margin growth. The wide and gently dipping mid-Norwegian margin facilitated coastal and shelf progradation related to fluvial and glacial processes, while the narrow and steep Lofoten–Vesterålen margin received little input from these sources although exposed to the same paleoclimate. Instead, erosion of canyons promoted downslope reworking across the slope and into the deep basins. This low sediment input is interpreted to be controlled by the alpine relief in the north resulting in a small source area and thus low fluvial and glacial sediment input. To the south, hinterland relief allowed for a much larger fluvial and later, glacial source area. Both margin segments were also influenced by contour currents throughout the studied period. We emphasize their importance for understanding the role of erosion and deposition in source-to-sink systems, and thus the need for these processes to be integrated within source-to-sink models.

### 1. Introduction

Passive continental margins at high northern latitudes are important Neogene–Quaternary sedimentary archives, as they are overlain by the global ocean conveyor belt and are close to major land-based ice sheets (e.g., Dahlgren et al., 2005; Rebesco et al., 2014). The margins have thus been under the influence of alongslope and downslope processes, which frequently erode, transport and deposit sediments. Typical characteristics of these northern margins include trough mouth fans (TMFs) and progradational wedges seaward of glacial outlet corridors (e.g., Vorren and Laberg, 1997; Dahlgren et al., 2005; Piper et al., 2012), as well as

contourite drifts and deep sea turbidite fans (e.g., Rebesco et al., 2014; Stow and Smillie, 2020). Such deposits are documented all along the Atlantic margin (Figs. 1a, 2a) (e.g., Eiken and Hinz, 1993; Dahlgren et al., 2005; Hernández-Molina et al., 2009; Ehlers and Jokat, 2013; Baeten et al., 2014; Mosher et al., 2017; Safronova et al., 2017; Lasabuda et al., 2018; Rydningen et al., 2020), and here we focus on the mid- to north-Norwegian continental margin between 64° and 69°N.

Ocean circulation similar to present day, where North Atlantic meridional overturning created favorable conditions for contourite drift growth (Viana et al., 2007), was likely established in the Norwegian–Greenland Sea between opening of Fram Strait ~17 Ma ago and

\* Corresponding author.

E-mail address: [stine.b.olsen@uit.no](mailto:stine.b.olsen@uit.no) (S. Bjordal-Olsen).

<https://doi.org/10.1016/j.margeo.2022.106974>

Received 28 April 2022; Received in revised form 13 December 2022; Accepted 19 December 2022

Available online 22 December 2022

0025-3227/© 2022 The Authors. Published by Elsevier B.V. This is an open access article under the CC BY license (<http://creativecommons.org/licenses/by/4.0/>).

subsidence of Greenland–Scotland Ridge at ~12 Ma (Fig. 1a) (Wright, 1998; Jakobsson et al., 2007; Rydningen et al., 2020). The establishment of the northern branch of the global conveyor belt is also believed to have had an important impact on paleoclimate as it led to heat and moisture supply to northern latitudes that allowed for ice sheet growth on land (Zachos et al., 2001; Smith and Pickering, 2003; Knies and Gaina, 2008; Eldevik and Nilsen, 2013). These ice sheets eroded the Scandinavian Peninsula, and thus increased sediment supply from the hinterland to the continental margin (e.g., Kleman et al., 2008; Dowdeswell et al., 2010; Mangerud et al., 2011; Patton et al., 2022). The

total volume of glacial sediments that accumulated on the mid-Norwegian margin during the Quaternary was estimated by Dowdeswell et al. (2010) and Hjelstuen and Sejrup (2021), and later revised by Lien et al. (2022); the latter calculated the total volume to be 114,000 km<sup>3</sup>, giving an average sedimentation rate of 0.73 m/k.y.

To understand how the continental margin evolved in response to this paleoclimatic development, the current study focuses on two morphologically different margin and basin segments: the mid-Norwegian region (64° to 68°N) and Lofoten–Vesterålen region (68° to 69°N). For the mid-Norwegian region, the hinterland morphology

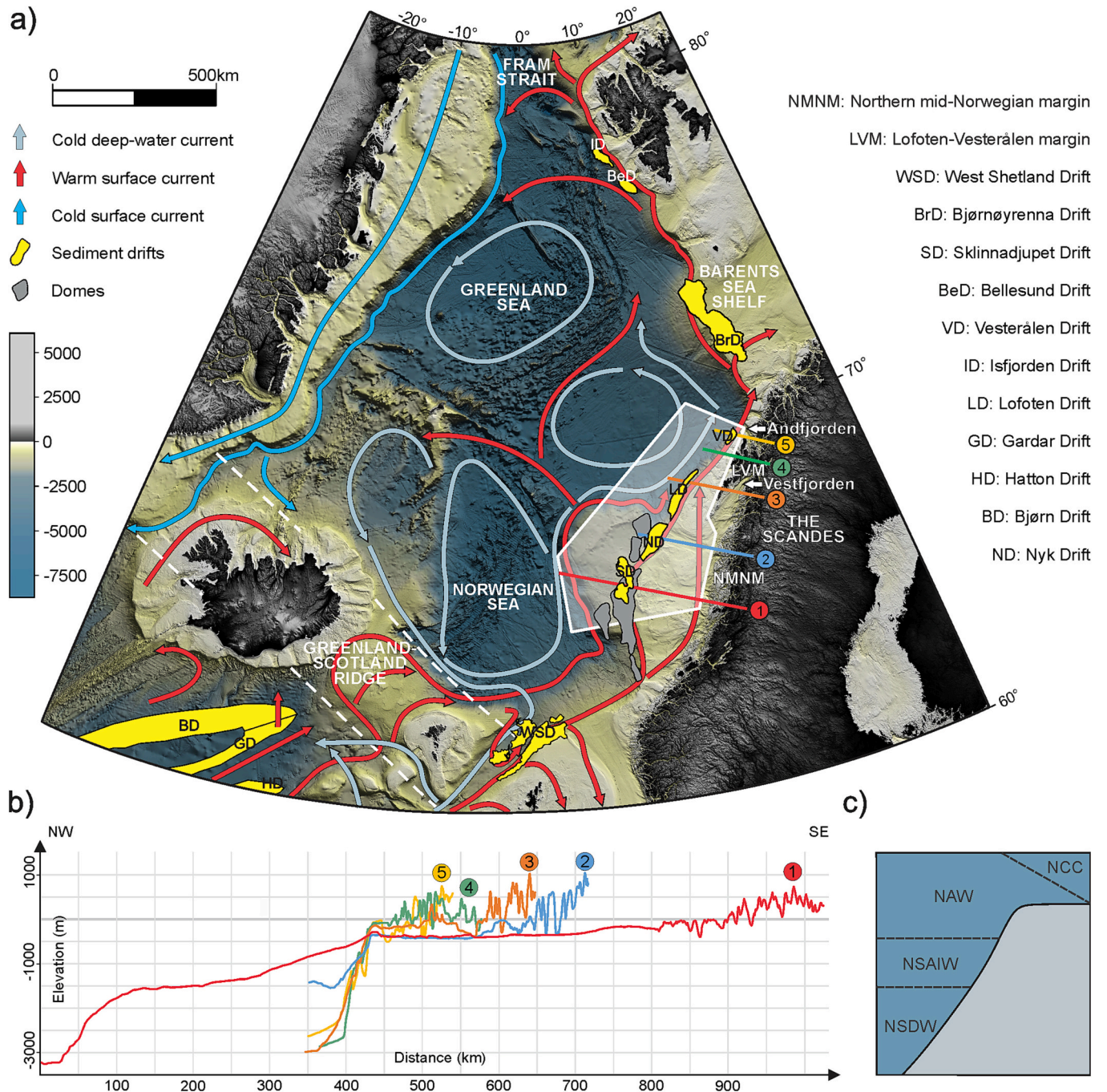


**Fig. 1.** a) Bathymetric map of the North Atlantic Ocean (GEBCO Compilation Group, 2019). Extent of contourites is according to Baeten et al. (2013) and the Flanders Marine Institute; Renard Centre of Marine Geology - UGent (2019), while the ocean circulation is from Hansen and Østerhus (2000) and Orvik and Niiler (2002). b) Bathymetric profiles, showing variations of margin morphology, including shelf width and slope gradient. See Fig. 1a for location of profiles. c) Distribution of water masses across the studied margin: NCC – Norwegian Coastal Current; NAW – Norwegian Atlantic Water; NSAIW – Norwegian Sea Arctic Intermediate Water; NSDW – Norwegian Sea Deep Water.



varies from low relief (<200 m; plateau) to high relief (up to c. 1000 m; alpine) (Fig. 1b, profiles 1, 2) (Corner, 2005; Ottesen et al., 2005). The adjacent margin has a >200 km-wide shelf and an upper slope that is gently dipping at c. 0–3° onto the Vøring Plateau in the west (Fig. 1b, profile 1) (Vorren et al., 1998; Laberg et al., 2001). In comparison, the Lofoten–Vesterålen region is dominated by high relief with elevations over 1000 m onshore (Fig. 1b, profiles 3–5) (Corner, 2005). A narrower shelf (minimum 6 km) and substantially steeper slope (up to 10°) is typical for the adjacent margin (Rise et al., 2013). These off-shore–onshore variations greatly influenced sediment transport routes and deposition (e.g., Dahlgren et al., 2005; Gołdowski et al., 2012; Newton and Huuse, 2017), of which resulted in variations of the sedimentation pattern along the margin through the Neogene and Quaternary, as will be elaborated in this study.

Previous studies in the area focused on smaller segments of the margin or on shorter time periods, e.g., Neogene contourite drift growth (Laberg et al., 2001; Bryn et al., 2005), Quaternary progradational wedge development (Henriksen and Vorren, 1996; Stuevold and Eldholm, 1996; Dahlgren et al., 2002; Rise et al., 2010; Montelli et al., 2018; Ottesen et al., 2022) and modern processes on the shelf (Vorren et al., 2015; Newton and Huuse, 2017). Consequently, the Neogene to Quaternary regional development of the northern mid-Norwegian and Lofoten–Vesterålen margin segments have not been well researched. This study will therefore determine the evolution of these contrasting margin segments (broad and gently sloping vs. narrow and steep sloping) by: i) construct the mid-Miocene–Quaternary (11–0 Ma)

seismic stratigraphy through analysis of seismic and exploration well data, ii) decipher major sedimentary processes responsible for construction of the stratigraphy and seafloor morphology, iii) determine climatic and tectonic forcing factors that controlled the antecedent morphology, sediment supply and the relative importance of along- and downslope processes. As a result of the observations in this study, a new class of contourite drifts is also proposed.

## 2. Background

### 2.1. Cenozoic continental margin evolution

The Norwegian continental margin formed because of breakup and seafloor spreading in the Norwegian–Greenland Sea, which started near the Paleocene–Eocene transition at ~55 Ma (e.g., Talwani and Eldholm, 1977; Eldholm et al., 1987; Faleide et al., 2008). This seafloor spreading set the stage for development of Fram Strait in the Miocene, and allowed for deep-water exchange between the previously isolated Arctic Ocean and Atlantic Ocean (Fig. 1a) (Kristoffersen, 1990; Jakobsson et al., 2007; Kaminski et al., 2009; Hutchinson et al., 2019). Timing of the North Atlantic–Arctic Ocean connection around 17 Ma, suggested by Jakobsson et al. (2007), coincided with the mid-Miocene Climatic Optimum, which culminated at c. 17–15 Ma, and was followed by gradual lowering of global temperatures (Zachos et al., 2001). Fram Strait did not reach modern water depths (>2 km) before at 13.7 Ma (Jakobsson et al., 2007), an age that is nearly synchronous with subsidence of

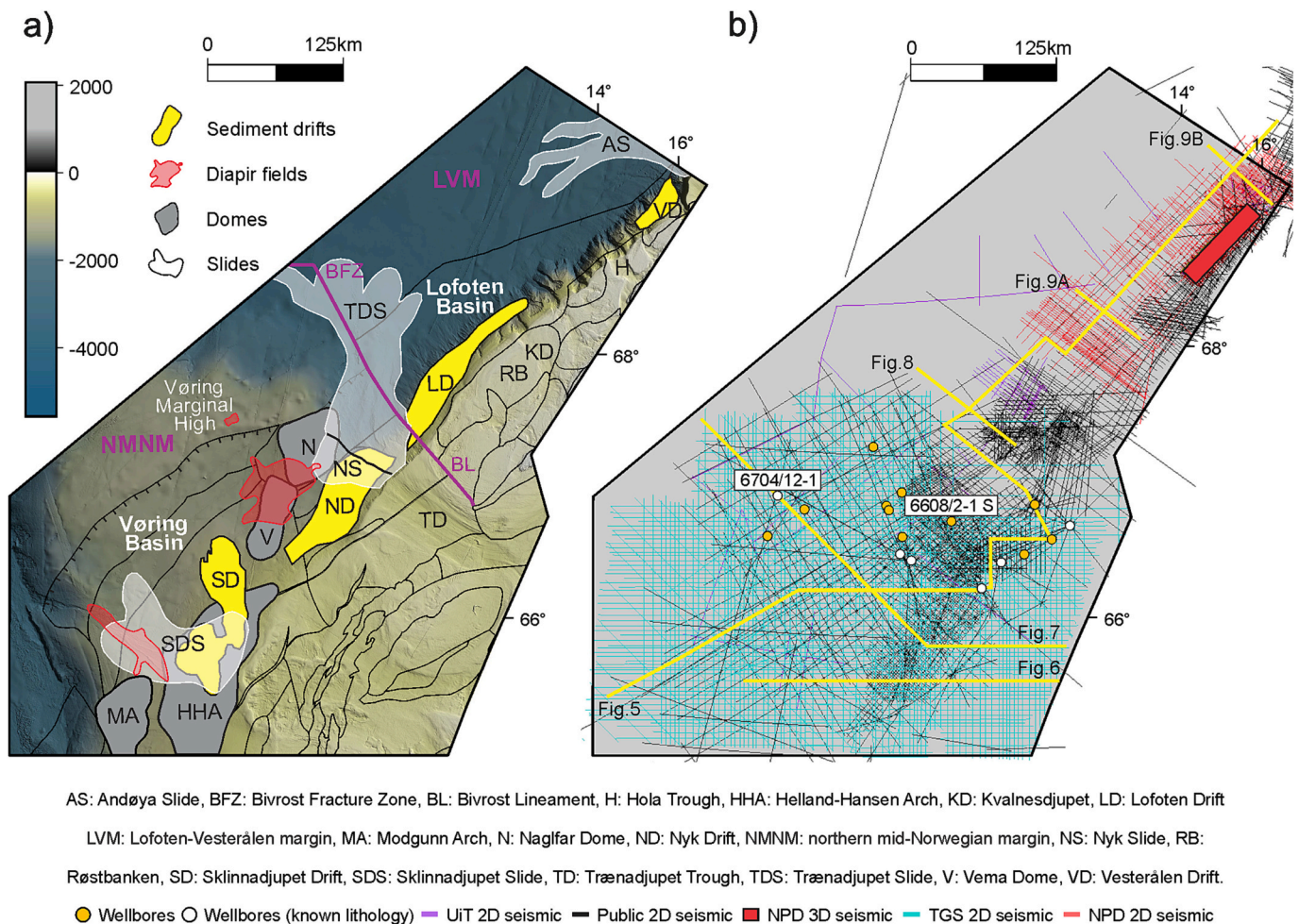


Fig. 2. a) Bathymetric map from IBCAO v. 4.0 (Jakobsson et al., 2020), including structural elements by the Norwegian Petroleum Directorate (Blystad, 1995). Extent of diapir fields and slides are from Hjelstuen et al. (1997, 1999), Laberg and Vorren (2000), Laberg et al. (2000) and Rise et al. (2006). b) Seismic data coverage and location of exploration wells.

Greenland–Scotland Ridge at c. 12 Ma (Fig. 1a) (Wright, 1998; Faleide et al., 2008). Subsidence of the ridge allowed for North Atlantic Deep Water to pass over this threshold and reach further north (Vogt, 1972; Laberg et al., 2001). These events strengthened ocean circulation responsible for drift growth in the North Atlantic from the Miocene (e.g., Wold, 1994; Hernández-Molina et al., 2003; Laberg et al., 2005; Stoker et al., 2005; Bellwald et al., 2022). Miocene drift sedimentation is also documented along continental margins around the globe, such as on the southern Mozambique margin (Preu et al., 2011), western Antarctica margin (Rebesco et al., 1997) and on the SE New Zealand margin (Fulthorpe and Carter, 1991).

In the early to middle Cenozoic, compression occurred along the NW European Atlantic margin; an event that caused basin inversion, reverse faults and formation of arches and domes on the mid-Norwegian margin (Fig. 1a) (e.g., Lundin and Doré, 2002; Stoker et al., 2005; Stephenson et al., 2020). These features formed along basin flanks, while uplift of the landward part of the margin caused formation of a mid-Miocene unconformity (Rise et al., 2010).

The mid-Cenozoic was also a period of northern hemisphere glaciations, as evidenced by Miocene ice-rafted debris (IRD) in boreholes on the western Iceland Plateau (Thiede et al., 1998). At Vøring Plateau further north, the oldest IRD are dated to 12.6 Ma but these deposits may have originated from the Greenland Ice Sheet, which expanded onto the Greenland Shelf at the time (Fronval and Jansen, 1996; Helmke et al., 2003). A notable increase in IRD, dated to 2.8 Ma, in boreholes on the northern mid-Norwegian margin is inferred to mark the onset of major north European glaciations (Jansen and Sjøholm, 1991; Fronval and Jansen, 1996). Glacigenic sediments sourced from Fennoscandia throughout this period increased the load on older unconsolidated muds and oozes, which triggered mud diapirism on the mid-Norwegian margin (Fig. 2a) (Hjelstuen et al., 1997, 1999). Polygonal faults probably acted as pathways for upward movement of sediment in this mud diapirism (Talwani and Eldholm, 1972; Hjelstuen et al., 1997).

During these glaciations, coastal highlands in the east controlled ice drainage and Fennoscandian ice masses were transported through Vestfjorden and Andfjorden (Fig. 1a). This routing prevented the main glacial drainage from reaching the Lofoten–Vesterålen shelf, where local ice domes instead drained to the shelf break during glacial maxima (Laberg et al., 2002; Ottesen et al., 2005; Vorren et al., 2015). Consequently, the glacial sediment input was lower for the Lofoten–Vesterålen segment compared with margin segments further north and south (Dowdeswell et al., 2010; Rydningen et al., 2016).

The Neogene–Quaternary sediment drainage pattern was affected by western Scandes, which acted as an important sediment source for the Norwegian Shelf (Fig. 1a) (Dehls et al., 2000; Eidvin et al., 2014). Two main hypotheses have been proposed for the origin of these mountains. The “classical” hypothesis emphasizes erosion to a peneplain followed by phases of Cenozoic uplift, signifying that the Scandes is a product of post-breakup uplift (Riis and Fjeldskaar, 1992; Riis, 1996; Lidmar-Bergström et al., 2000; Japsen et al., 2018). For this hypothesis, uplift phases are assumed to explain increased sedimentation in adjacent basins (Pedersen et al., 2018). The ICE (isostasy, climate, erosion) hypothesis, on the other hand, emphasizes gradual erosion and simultaneous isostatic uplift of existing topography, indicating that Scandes is a remnant from the Caledonian Orogeny rather than a product of Cenozoic uplift. For this view, enhanced sedimentation is suggested to be a result of climate-related increase in erosion rate (Nielsen et al., 2009; Pedersen et al., 2016, 2018).

## 2.2. Morphology of the Norwegian continental margin

The continental shelf is >200 km wide on the mid-Norwegian margin, and between 6 and 90 km wide on the Lofoten–Vesterålen margin (narrowing northwards) (Vorren et al., 1998, 2015; Rise et al., 2013). These shelf areas comprise shallow banks and deeper transverse troughs, usually ranging down to water depths of 250–500 m and

50–200 m for the mid-Norwegian and Lofoten–Vesterålen shelf, respectively (Vorren et al., 1998).

The mid-Norwegian slope dips gently westwards (0–3°) onto the Vøring Plateau, situated at 1200 to 1400 m water depth. On the outer plateau, the slope dips more steeply into abyssal plains of the Norwegian and Lofoten basins (Fig. 2a) (Laberg et al., 2001, 2005). The Lofoten–Vesterålen slope is the steepest on the Norwegian margin with slope gradients up to 10° (Fig. 1b, profiles 3–5).

The slope morphology is dominated by a progradational wedge in the mid-Norwegian region, and alternating contourite drifts and canyons on the Lofoten–Vesterålen slope (Vorren et al., 1998; Dahlgren et al., 2005; Buhl-Mortensen et al., 2010; Rise et al., 2013). The largest contourites are the Sklinnadjupet, Nyk, Lofoten and Vesterålen drifts (Laberg et al., 1999, 2001). North of the study area, offshore northern Norway, TMFs are documented at the outlet of cross-shelf troughs (Dahlgren et al., 2005; Rydningen et al., 2015, 2016). Vast submarine landslide scars across the study area include the Sklinnadjupet, Nyk, Trænadjupet and Andøya slides (Fig. 2a) (Vorren et al., 1998; Laberg and Vorren, 2000; Laberg et al., 2000; Evans et al., 2005; L'Heureux et al., 2013; Laberg et al., 2016).

## 2.3. Modern and Quaternary oceanography

Four water masses dominate the modern continental shelf and slope off Norway: Norwegian Coastal Current Water, Norwegian Atlantic Water, Norwegian Sea Arctic Intermediate Water and Norwegian Sea Deep Water (Fig. 1c). The low-salinity Norwegian Coastal Current originates in the Baltic Sea and flows along the coast while receiving run-off from rivers, and continues into the Barents Sea (Buhl-Mortensen et al., 2010, 2012). Beneath and to the west of this current is the warm and highly saline Norwegian Atlantic Water of the Norwegian Atlantic Current (Buhl-Mortensen et al., 2010). This current is a two-branch system, with a western branch flowing from the Iceland–Faroe Front towards Fram Strait, and an eastern branch flowing through the Faroe–Shetland Channel and northwards along the Norwegian shelf edge (Fig. 1a) (Orvik and Niiler, 2002). This oceanography contrasts with the circulation in the North Atlantic during Quaternary glacial periods (Laberg et al., 2005), when an increased flux of icebergs and meltwater caused low temperature and low salinity water to overlie warmer and saltier Norwegian Atlantic Water (Rasmussen et al., 1997, 2014). This structure enhanced formation of intermediate water masses at the expense of deep water (Boyle and Keigwin, 1987; Rasmussen et al., 2003b). Deep-water circulation was therefore reduced during glaciations, while it strengthened during interglacial periods and after LGM (McCave et al., 1995).

## 2.4. Seismic stratigraphic framework

The studied interval covers the Kai, Molo and Naust formations (Fig. 3). Kai and Molo formations have been mapped previously only in the northern mid-Norwegian region, where Kai Formation consists of mud grading into siliceous and calcareous oozes in the deep basins. Samples near its base have ages of ~11 and ~9.6 Ma (Eidvin et al., 2007). The Molo Formation contains sandy clinoforms, and for decades its age has been debated due to lack of reliable age constraints (Henriksen and Weimer, 1996; Eidvin et al., 2007; Løseth et al., 2017; Grøsfjeld et al., 2019; Eidvin et al., 2022). Recently, Grøsfjeld et al. (2019) proposed that the lower and northernmost part of the formation (well 6610/3–1) began to accumulate ~8.8–8.7 Ma ago. This age compares well with the late Miocene age suggested by Dybkjær et al. (2020) for the lowest and southern Molo Formation (well 6407/9–5). Despite these new results, there are still debates about the age of Molo Formation (Løseth, 2021).

Naust Formation consists of a glacigenic progradational wedge of contouritic, glacialmarine and mass-transport deposits in the northern mid-Norwegian region, while it is contourite-dominated in the



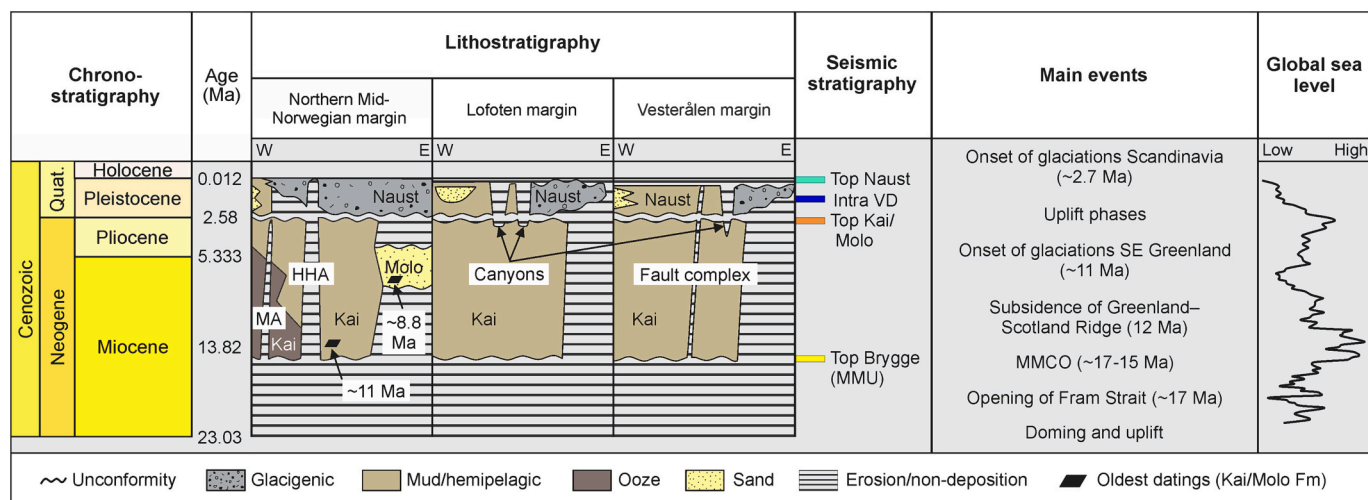


**Fig. 3.** Seismic-, litho- and chronostratigraphy for the northern mid-Norwegian and the Lofoten–Vesterålen margin. Lithostratigraphy is modified from Eidvin et al. (2019), while the geological timescale follows Cohen et al. (2016). HHA – Helland-Hansen Arch; Intra VD – Intra Vesterålen Drift; MA – Modgunn Arch; MMCO – Mid Miocene Climatic Optimum; MMU – Mid-Miocene Unconformity. Global sea level curve is from Miller et al. (2020).

Lofoten–Vesterålen region (Dahlgren et al., 2002, 2005; Ottesen et al., 2009). Eidvin et al. (2020) investigated a sample from the upper Naust “N” (well 6507/5-J-1 H), just above our mapped top Kai/Molo horizon, giving an age between 1.7 and 1.4 Ma. However, Ottesen et al. (2009) tentatively suggested an age between ~2.7 and ~1.5 Ma for the oldest Naust “N” unit, while Dahlgren et al. (2002) interpreted the base of their seismic unit “D” (corresponding to seismic unit “A” overlying Naust “N”) of Ottesen et al. (2009) to be ~0.9–1.1 Ma.

### 3. Data and methods

The seismic database comprises 2D seismic surveys acquired since the 1980’s, most of which are downloaded from the Norwegian Petroleum Directorate (NPD) DISKOS database (Fig. 2b). Newer multichannel 2D lines (NPD-LOF1–07/08) and one 3D survey (NPD-LOF1–09) acquired by the NPD between 2007 and 2009 were also studied. In addition, the database includes unpublished multichannel 2D lines collected by TGS (MNRO4–11) from 2004 to 2011, as well as single-channel 2D lines acquired by UiT The Arctic University of Norway, between 2000 and 2003 and 2010, with R/V *Jan Mayen* (now R/V *Helmer Hanssen*).

The seismic data coverage is best in the central shelf/upper slope area on the northern mid-Norwegian margin, offshore southern Lofoten and over the shelf/upper slope off Andøya, with an average line spacing between 1 and 2 km (Fig. 2b). The line spacing increases to 3–6 km over the lower slope off Lofoten–Vesterålen, while the sparsest coverage is in the western Lofoten Basin (up to 65 km). The overall quality of the seismic data is good, but the older surveys are of lower quality with seabed multiples. Vertical resolution at a depth of 2000–2500 ms two-way travel time (TWT) for the Kai Formation near well 6704/12–1 is ~11 m (Fig. 2b). This was calculated by using an average interval transit time of ~1550 m/s from the sonic log at a frequency of ~35 Hz (from seismic data) and assuming the Rayleigh criteria of 1/4 wavelength as limit of resolution. Further east, in well 6608/2–1 S, the transit time and dominant frequency at a depth of c. 1900–2100 ms TWT is ~3390 m/s and ~15 Hz, which gives a vertical resolution of ~56 m for the Kai Formation (Fig. 2b). The poorer resolution in the east may be related to the thick overlying Naust wedge here, causing compaction and higher velocities.

Seventeen exploration wells in the mid-Norwegian region were used to provide age and lithological control (Fig. 2b). These wells were chosen because they contain information about the Neogene–Quaternary sediments and form a E-W transect from shelf to basin areas. Formation tops in the wells (downloaded from <http://factpage.npd.no>) form the main basis for the established seismic stratigraphy,

although mismatch between picks in different wells occur occasionally. Nevertheless, confidence of stratigraphic constraints is not reduced because of correlation between several wells. Age constraints were obtained through correlation to wells and dating results from previous work, such as Eidvin et al. (2007), Grøsfjeld et al. (2019), Dybkjær et al. (2020) and Eidvin et al. (2020). We refer to these publications for further discussions on age determinations. Stratigraphic and age constraints become less reliable towards the Lofoten–Vesterålen region because no deep-target exploration wells are present, and because seismic correlation is complicated by diapiric fields, slides and complex structural elements (Fig. 2a). Uncertainties also exist concerning well-to-seismic ties because of the large resolution difference between these data sets. Moreover, when interpreting seismic in the Vøring Basin, diagenetic bottom simulating reflectors must be avoided (e.g., Hjelstuen et al., 2004; Chand et al., 2011). These reflectors are positive moderate to high amplitude reflections that crosscut bedding.

Three key seismic horizons were mapped: 1) top Brygge, bounding the Brygge and Kai/Molo formations, 2) top Kai/Molo, separating the Kai/Molo and Naust formations and 3) top Naust, seafloor horizon (Fig. 3). Horizon mapping also included an intra-Vesterålen Drift horizon (separating top Kai/Molo and top Naust). The term “mid-Miocene unconformity”, identified in other studies as the base of the Kai and Molo formations (e.g., Løseth and Henriksen, 2005; Eidvin et al., 2007; Løseth et al., 2017), is not used in this study. However, based on its seismic character and stratigraphic depth, it is inferred to correspond to our top Brygge horizon.

Completion reports from available wells contain information on the lithology of the Kai, Molo and Naust formations, based on interpretations of sidewall cores, cuttings, core samples, and wireline logs. Six wells were used for lithological characterization: 6610/3–1, 6609/5–1, 6609/7–1, 6607/5–1, 6607/5–2 and 6704/12–1 (Table 1).

## 4. Results

### 4.1. Seismic facies

Four seismic facies (SF1–4) are recognized and classified for the study area based on the terminology defined in Mitchum et al. (1977) and Badley (1985) (Fig. 4). Low to medium amplitude and continuous to semi-continuous inclined reflections up to c. 13° characterize SF1A (tangential oblique). These reflections are typically truncated in the top and they have downlap terminations onto the lower boundary. SF1B (tangential oblique) has a similar reflection configuration and

**Table 1**

Lithology from six exploration wells of the interval covering the Kai, Molo and Naust formations. The wells are listed systematically from the inner shelf in the east to the deeper Vøring Basin in the west. For location, see Fig. 2b.

	Naust	Molo	Kai
6610/3-1	17 m. Sediments ranging from clay to gravel.	206 m. The upper 111 m contains sand/sandstone, while the 95 m long interval underneath becomes siltier and more clayey. Limestone stringers occur in the lowermost 35 m.	Not present.
6609/5-1	1252 m. Claystone/clay with sand stringers.	Not present.	177 m. Claystone with lime- and sandstone stringers.
6609/7-1	1125 m. The upper 325 m contains gravels, unconsolidated sands and claystones. The clay content increases downward. The clays are interbedded with thin layers of unconsolidated sands. A further rise in claystone content is apparent in the lowermost 375 m.	Not present.	60 m. Claystone.
6607/5-1	1820 m. Claystone with minor sand laminae and occasional silty-sandy beds.	Not present.	250 m. Claystone with minor sand lamina.
6607/5-2	1454 m. Claystone with thin sandstone interbeds.	Not present.	314 m. Claystone interbedded with thin sandstone stringers.
6704/12-1	82 m. Soft to very soft clay grading to firm clay towards the lower part.	Not present.	461 m. Silica ooze with minor clay content.

terminations, but the reflections slope at a gentler angle (c. 1–3°), and their amplitudes range between medium to high. A wedge shape is common for deposits that comprise these facies. The contorted facies (SF2) is dominated by low to high amplitude, continuous divergent reflections. These reflections typically have onlap terminations facing towards the east, and downlap terminations oriented to the west. Incisions occur frequently in association with the upslope onlap terminations, and a mounded external form is typical. SF3 contains low to high amplitude, continuous to semi-continuous, parallel to sub-parallel reflections with onlap terminations. These reflections commonly have an external sheet geometry. Low to high amplitude, discontinuous chaotic reflections characterize SF4. A transparent matrix is typical together with an irregular top and base.

#### 4.2. Top Brygge horizon characteristics

The top Brygge horizon is a continuous, high amplitude and negative polarity reflection that truncates underlying strata (Figs. 5–9). However, in the northeastern mid-Norwegian region where it separates the Brygge and Molo formations, it is discontinuous (Fig. 6). Faults are observed in the Brygge Formation and the majority of these terminate near the top Brygge horizon, although a few also penetrate it (Figs. 6–9).

The top Brygge horizon is a regional northwestward dipping paleosurface (Fig. 10a). In the northern mid-Norwegian region, it has been mapped from the inner shelf in the east and ~400 km seaward. Within the Vøring Basin, it slopes generally <3°. Here, the horizon outlines two paleobasins (reaching depths of >3700 ms TWT), separated by a SE-NW oriented ridge. Elsewhere in this area, smaller S-N and SW-NE oriented structural highs, ridges and domes characterize the horizon. In the Lofoten–Vesterålen region, the top Brygge horizon was identified in a smaller area (up to ~165 km wide) that includes the slope and parts of the Lofoten Basin (Fig. 10a). The horizon is absent on the shelf where it is truncated by the seafloor, while westward it lies on a steeply dipping slope (up to ~13°) incised by SW-NE-aligned gorges (Table 2 and Figs. 9a, 10e).

#### 4.3. Kai Formation character and age

Elongated mound-shaped accumulations with an alongslope SSW–NNE direction fill in the confined areas between ridges and domes in the eastern part of the mid-Norwegian region (Fig. 10b). These accumulations (I–III, Table 3) are up to ~280 km long, 110 km wide and

~455 ms TWT thick (Figs. 6a, 11a). Their internal reflection configurations are dominated by SF2, that is, a contorted seismic signature with onlap terminations onto underlying domes, highs and ridges. Similar accumulations (IV–VII, Table 3) are present in the deeper Vøring Basin to the west, where they reach thicknesses up to ~960 ms TWT (Fig. 7). The Kai Formation here also includes intervals of SF3 (parallel to sub-parallel), reaching thicknesses up to ~300 ms TWT. These sediments are in some places truncated by the base Naust horizon, particularly in the shallow area of the SE-NW oriented ridge. Low-displacement polygonal faults also affect Kai Formation in the western and northern Vøring Basin.

In the Lofoten–Vesterålen region, just north of the Bivrost lineament, the Kai Formation is absent in the modern shelf setting where it is truncated (Figs. 9c, 10b). Downslope oriented accumulations, internally dominated by SF3 (parallel to sub-parallel), characterize the upper slope. Further downslope, SF3 is interbedded with SF4 (chaotic). Areas of thinner or absent Kai deposits separate the downslope accumulations on the slope (Figs. 8, 10b). In the southern Lofoten Basin, the formation is between ~70 and 490 ms TWT thick and mainly comprises SF2, that is, a contorted reflection configuration (VIII, Table 3) (Fig. 11a). The reflections here have a similar low-displacement fault pattern as in the Vøring Basin, although it is less prevalent (Fig. 8). Towards the northern parts of Lofoten Basin, off Vesterålen, the formation thickens to a maximum of ~950 ms TWT and is characterized by an internal signature dominated by SF2 and SF4 (Fig. 9b). SF2 is mostly confined to an accumulation along the eastern basin margin that onlaps underlying strata (IX, Table 3), while SF4 dominates seaward (Figs. 9f, 11a). Compared with the northern mid-Norwegian elongated accumulations, the Lofoten–Vesterålen accumulations have a smaller areal extent and onlap a steeper slope incised by gorges (Figs. 8, 10b).

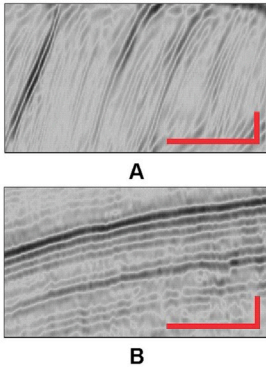
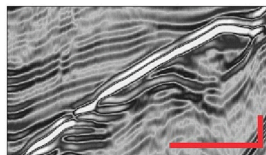
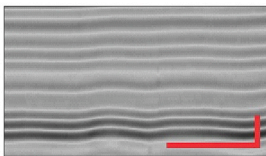
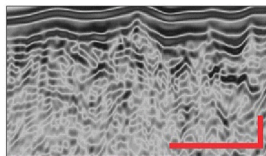
Seismic correlation to biostratigraphic interpreted ages of the 6607/5-1 well, near the base of the Kai Formation, show that the formation started to accumulate in the northern mid-Norwegian region just prior to c. 11 Ma, in the late Miocene.

Samples taken further up in the well show that the formation continued to accumulate at least until 6.9–5.1 Ma (Eidvin et al., 2007).

#### 4.4. Molo Formation character and age

Molo Formation is located on the inner mid-Norwegian shelf (65°–67°40'N), and it is ~300 km long, between 7 and 55 km wide, up



Seismic Facies (SF)	Description
<p><b>SF1 – Tangential oblique</b></p> 	<p>Steeply (up to <math>\sim 13^\circ</math>) inclined and continuous to semi-continuous reflections of low to medium amplitude. Often truncated in the upper part. Sand-rich lithology is common (e.g., Eidvin et al., 2007).</p> <p>Gently inclined and continuous-semi continuous reflections of medium to high amplitude. Commonly truncated in the top. Typically composed of varying lithologies, ranging from clay to gravel (e.g., Rokoengen et al., 1995).</p>
<p><b>SF2 – Contorted</b></p> 	<p>Low to high amplitude, continuous divergent reflections with progressive upslope onlap terminations. Incisions often occur in association with the onlap. Mud-rich lithology is common (e.g., Faugères and Stow, 2008; Rebesco et al., 2014).</p>
<p><b>SF3 – Parallel to sub-parallel</b></p> 	<p>Low to high amplitude, continuous to semi-continuous, parallel to sub-parallel reflections. A fine-grained lithology is common, typically muds and sandy muds (e.g., Stow and Smillie, 2020).</p>
<p><b>SF4 – Chaotic</b></p> 	<p>Low to high amplitude, discontinuous chaotic reflections. Transparent matrix common in some areas. Irregular top and base. Varying lithologies are common (e.g., Laberg et al., 2006; Bull et al., 2009).</p>

**Fig. 4.** Seismic facies classification. Red vertical and horizontal bars represent 50 ms TWT and 1 km. (For interpretation of the references to color in this figure legend, the reader is referred to the web version of this article.)

to  $\sim 520$  ms TWT thick, and wedging out north of the Bivrost Lineament (Figs. 6b, 7, 10b, 11a). The formation is characterized by SF1A (tangential oblique facies). A prominent truncation of SF1A by the seafloor or internal Naust unconformities is observed in the east (Fig. 6b). In central Trænadjupet, west of where the formation reaches its maximum thickness, the formation continues downslope and inter-fingers with the upper part of the Kai Formation (Figs. 5, 10b).

Seismic correlations to biostratigraphic age constraints near the base of the Molo Formation (well 6610/3–1) show that it started accumulating in the late Miocene at  $\sim 8.8/8.7$ , and continued into the early Pliocene (wells 6407/9–1/9–2/9–5) (Eidvin et al., 2007; Grøsfjeld et al., 2019; Dybkjær et al., 2020).

#### 4.5. Top Kai/Molo horizon characteristics

The top Kai/Molo horizon is a continuous high-amplitude negative reflection that represents an angular unconformity, which separates the Molo and Kai formations from Naust Formation (Figs. 7, 9a). In the northern mid-Norwegian region, the horizon is a gently westward dipping paleo-surface (up to  $\sim 3^\circ$ ) that is up to 400 km wide and displays a

shallowing trend towards the east (Table 2 and Fig. 10c). Around the Helland-Hansen Arch, it is truncated while elsewhere in the Vøring Basin it partly mimics the top Brygge horizon, outlining two basins separated by a NW-SE ridge.

The mapped area of the top Kai/Molo horizon in the Lofoten–Vesterålen region narrows from 290 km off southern Lofoten to 100 km off Andøya. Here, it represents an up to  $12^\circ$  NW dipping paleo-surface incised by deep gorges (Table 2 and Figs. 10c, f). Steepest gradients occur on the upper slope and in connection with gorge sidewalls, while the horizon dips more gently on the lower slope ( $0.5\text{--}3.5^\circ$ ). At the slope offshore Vesterålen, the horizon is partly truncated (Fig. 10c). West of the slope, the top Kai/Molo horizon is deep and gently sloping ( $<0.5^\circ$ ) within the region of the Lofoten Basin (Table 2 and Fig. 2a).

#### 4.6. Naust Formation character and age

Naust Formation is thin or absent on the inner northern mid-Norwegian shelf but the thickness increases progressively westward, reaching a maximum of  $\sim 1800$  ms TWT along the modern shelf break (Fig. 10d). In this area, the formation has an external wedge shape that

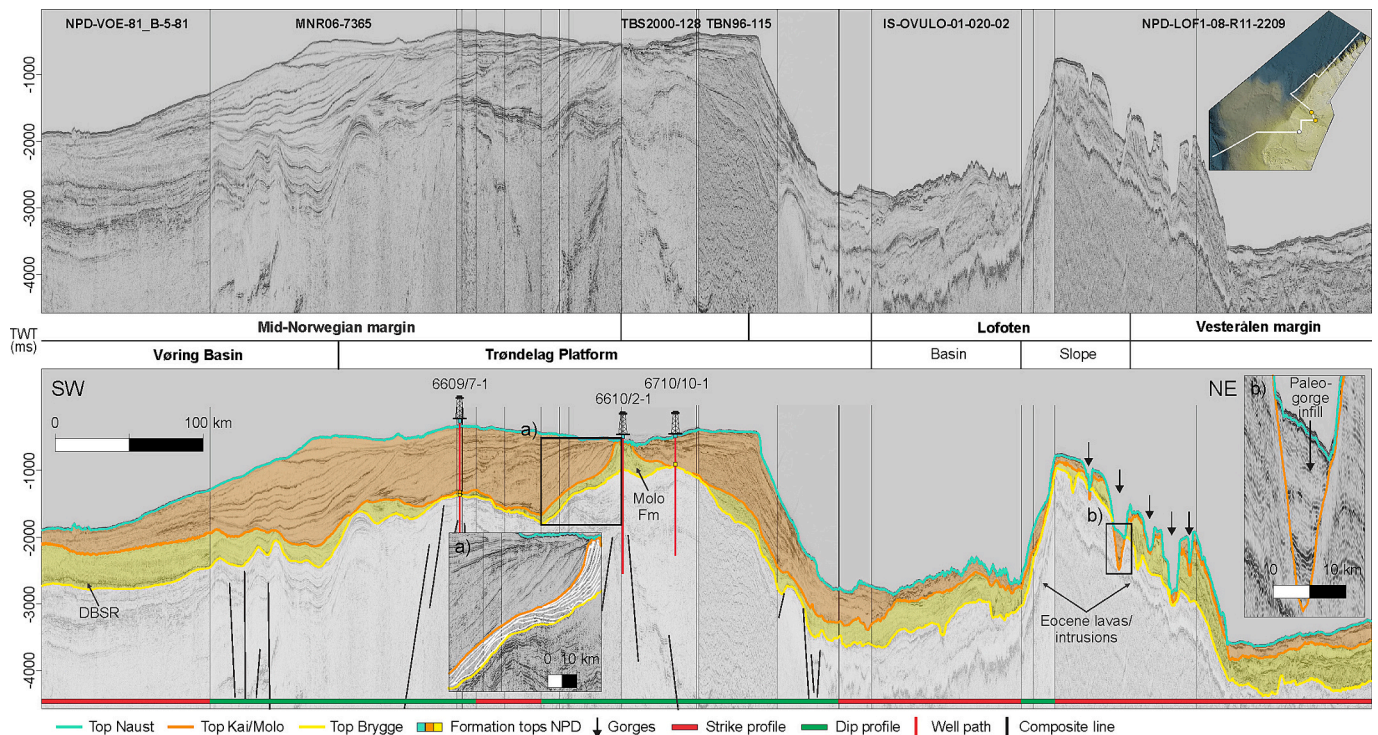


**Fig. 5.** Composite line across the study area displaying the regional extent of the Kai, Molo and Naust formations. DBSR – Diagenetic bottom simulating reflector. a) Stratigraphic relationship between Molo and Kai formations. Molo Formation continues downslope and into the deeper Kai Formation. b) Partly infilled canyon. See Fig. 2b for location.

internally is dominated by SF1B (tangential/oblique facies). Truncation of SF1B is observed east of the shelf break and younger strata with a parallel reflection configuration (SF3) rest on this unconformity (Figs. 6, 7). In the west, SF1B reflections downlap onto the underlying Kai and Brygge formations. The wedge also comprises intervals of SF2 and SF4, i. e., a contorted to chaotic seismic signature. The seismic stratigraphy of the Naust wedge off mid-Norway and its age between 2.7 and 0 Ma is described in detail in previous work (e.g., Dahlgren et al., 2002, 2005; Rise et al., 2006; Ottesen et al., 2009).

In the distal and western Vøring Basin, the Naust Formation wedge pinches out (Figs. 7, 10d). The thickest deposits fill the two sub-basins of the underlying top Kai/Molo horizon (~450 ms TWT thick) (Table 2 and Fig. 10d). The southernmost accumulation lies within the Sklinnadjupet Slide and the Vigrid diapir field, while the northern depocenter coincides with the Vema diapir field (Figs. 2a, 10d). Both depocenters are dominated by SF3 (parallel to sub-parallel) and SF4 (chaotic), and have been described thoroughly by Rise et al. (2006) and Hjelstuen et al. (1997, 1999). Along the western flank of Helland-Hansen Arch, the lowest interval of the Naust Formation (accumulation X, Table 3) has a mounded geometry dominated by an internal contorted signature (SF2) that onlaps the arch (Figs. 6, 11b). Thinning of the formation occurs over the NW-SE-oriented ridge that separates the sub-basins of the Vøring Basin, where SF3 dominates (Figs. 7, 10d). Polygonal faults, some extending to the seafloor, affect parts of the deposits within the basin.

The formation is thinner (up to ~1100 ms TWT) in the Lofoten–Vesterålen region north of the Bivrost lineament, and it is mostly absent or below data resolution on the shelf. Two elongated and along-slope oriented accumulations dominate on the slope (LD and VD; Table 3 and Figs. 10d, 11b). These accumulations are up to ~110 km long, 35 km wide and ~770 ms TWT thick. They have an external mounded geometry with an internal signature characterized by SF2 (contorted) that onlaps the underlying steep slope incised by gorges (Figs. 9a, b). SF2 are in some areas interbedded with intervals of SF4 (chaotic). These two accumulations outline the detailed extent of the Lofoten and Vesterålen drifts (Figs. 10d, 11b) (Laberg et al., 1999, 2001).

Near the outlet of the Hola, Kvalnesdjupet, and Andfjorden troughs, the Naust Formation is characterized by northwestward inclined reflections of SF1B (tangential/oblique) that partly fill in gorges on the upper slope (Figs. 1a, 2a, 9a). The thickness of these systems is between ~540 and ~1080 ms TWT. On the lower slope and in Lofoten Basin, Naust Formation displays thick accumulations in the continuation of the gorges (Fig. 10d). In the area of the Trønadjupet Slide deposits (Fig. 2a), the formation is up to ~490 ms TWT thick and dominated by SF4 (chaotic) with an irregular upper boundary (Fig. 5) (see Laberg and Vorren (2000) for more details on the slide). Further north in Lofoten Basin, the formation is thinner and dominated by SF3 (parallel to sub-parallel) (Fig. 10d). Off Vesterålen, the slope-basin transition is characterized by a major fault system (Fig. 9b). West of this system, a series of depocenters are present in Lofoten Basin downslope of the gorges (Fig. 10d). These depocenters mainly consist of SF3 interbedded with SF4 (Fig. 9b). SF3 is confined to an accumulation (XI, Table 3) on the eastern basin margin (Fig. 11b). Upslope, this facies changes to SF2, with a mounded geometry, divergent reflections and onlap terminations on the steep slope (Fig. 9b).

## 5. Discussion

### 5.1. Evidence of depositional pattern and sedimentary processes from seismic facies

The sediment bodies characterized by seismic facies SF1A (tangential oblique; steeply inclined reflections) have an external wedge shape and a sandy lithology (e.g., as shown in well 6610/3-1), indicating a coastal deltaic paleoenvironment that formed progradational wedge deposits (Table 1 and Fig. 4), as also concluded by others (e.g., Rokoengen et al., 1995; Henriksen and Vorren, 1996; Eidvin et al., 2007, 2019). The more gently inclined reflections of SF1B (tangential oblique) covers a larger region, has a greater volume, and is composed of a coarser lithology (e.g., gravels in wells 6610/3-1 and 6609/7-1). These features are indicative of a glacial marine paleoenvironment that formed progradational



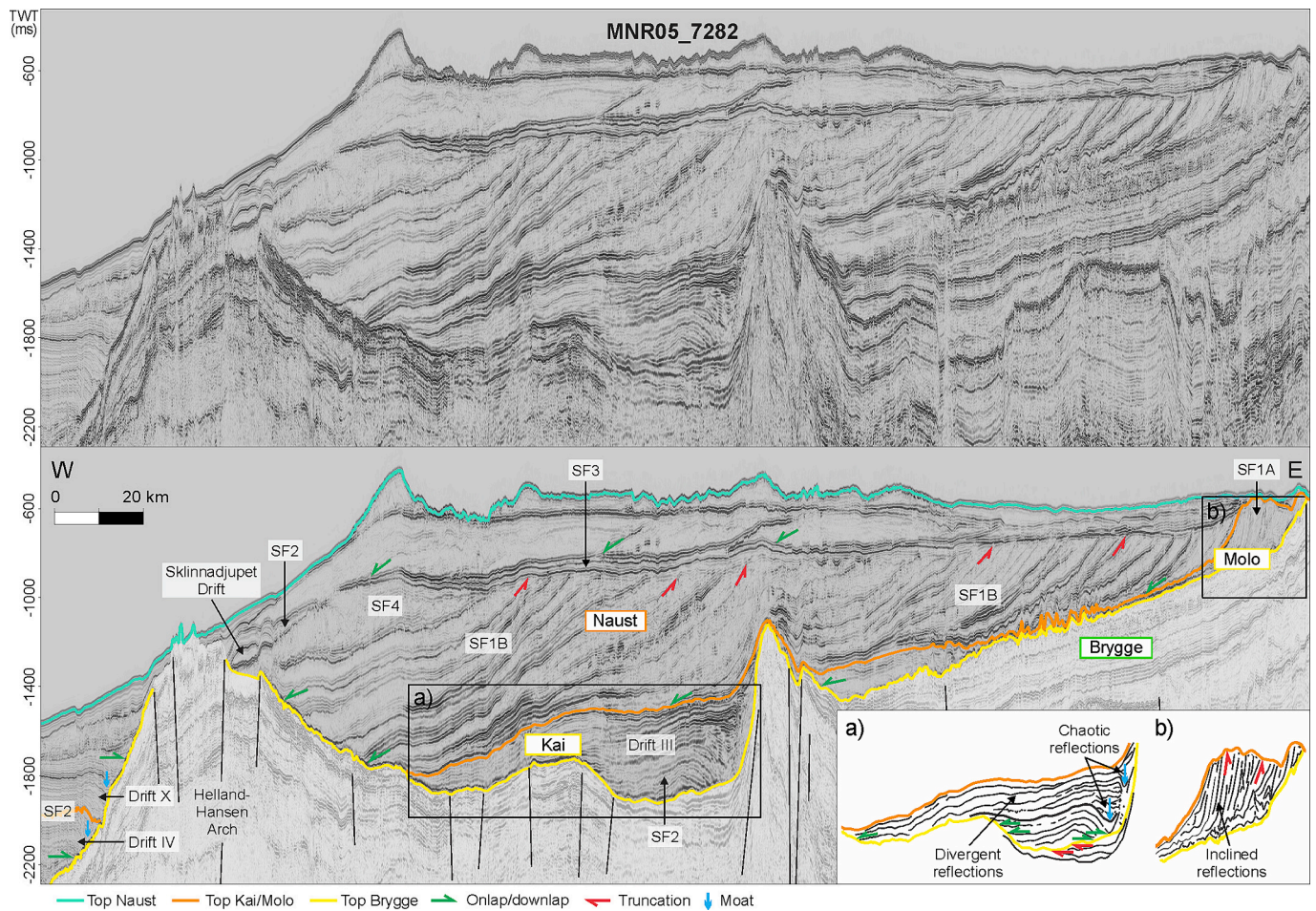


**Fig. 6.** Seismic dip profile across the northern mid-Norwegian margin. a) SF2 dominates the Kai Formation that onlap underlying domes. b) SF1A characterizes the Molo Formation that displays a downlap relationship to underlying strata, while it is truncated in the top. See Fig. 2b for location.

wedge deposits of various origins, as detailed in previous works from the mid-Norwegian region (e.g., Dahlgren et al., 2005; Rise et al., 2005; Ottesen et al., 2009).

Divergent reflections with onlap terminations (SF2), an external mounded elongated geometry and clay-rich lithology (e.g., piston core samples in well 6609/5-1 (Laberg and Vorren, 2004; Baeten et al., 2014)), are interpreted to be contourite drifts (I–XI, SD, ND, LD, VD; Table 1 and Figs. 4, 11). Drifts are formed by alongslope flowing contour currents that generally transport fine sand or smaller grain fractions, and favor elongation in a slope-parallel direction (e.g., Faugères et al., 1999; Faugères and Stow, 2008; Rebesco et al., 2014). They form asymmetrical, mounded accumulations with deposition on one side and erosion on the other where the flow is focused (e.g., Rebesco et al., 2014; de Castro et al., 2021; Miramontes et al., 2021). Incisions that are observed in association with the upslope onlaps are interpreted to be moats, i.e., areas of higher flow velocities and erosion. A selection of the drifts is penetrated by wells, and it is therefore reasonable to infer a clay-rich lithology for the contourites. The results from our seismic mapping reveal for the first time outline of drifts I–XI within the Neogene–Quaternary succession on the Norwegian margin, while outlines of the Skiinnadjupet, Nyk, Lofoten and Vesterålen drifts are updated.

The widespread distribution and fine-grained lithology (e.g., silica ooze in well 6704/12-1) (Table 1) together with the parallel to sub-parallel reflection configuration of SF3 are indicative of hemipelagic to pelagic deposits that have settled out from suspension during glacial and interglacial periods (Fig. 4). Hemipelagic to pelagic sediments often form in distal deep-water settings where other processes are absent or rare, and reflect a low-energy environment with fine-grained lithologies

(e.g., Stow and Smillie, 2020).

The chaotic reflection configuration of SF4, together with their irregular base and top, indicating erosional surfaces, are interpreted to be deposits from mass-transport processes such as slides, slumps and debris flows, commonly termed mass-transport deposits (Fig. 4) (e.g., Laberg et al., 2006; Tripsanas et al., 2008; Bull et al., 2009). Such deposits are gravity-induced and favor elongation in a downslope direction (e.g., Faugères et al., 1999; Nielsen et al., 2008; Nugraha et al., 2020; Wu et al., 2020).

## 5.2. Evolution of the northern mid-Norwegian and the Lofoten–Vesterålen regions

### 5.2.1. Early to mid-Miocene (older than ~11 Ma to ~8.8/8.7 Ma)

The top Brygge horizon possibly formed due to uplift of the shelf and landward part of the margin during early to middle Cenozoic compression (Rise et al., 2010). This compression resulted in the formation of domes, highs and arches in the Vøring Basin that was later onlapped by contourites in the Kai Formation (Fig. 6). A depositional hiatus also developed due to erosion related to this event, as indicated by the lack of sediments of lower to mid-Miocene age (Fig. 3). Faults that penetrate the horizon may be ascribed to Paleogene rifting that led to opening of Norwegian–Greenland Sea (Figs. 6–9).

Contourites in the Kai Formation off mid-Norway have earlier been described in very general terms (e.g., Bruns et al., 1998; Hjelstuen et al., 2004; Bryn et al., 2005), while in the current study they are properly defined (I–VII, Table 3 and Fig. 11a). The top Brygge horizon, that marks the base of the drifts, is overlain by c. 11 Ma Kai deposits in the west and



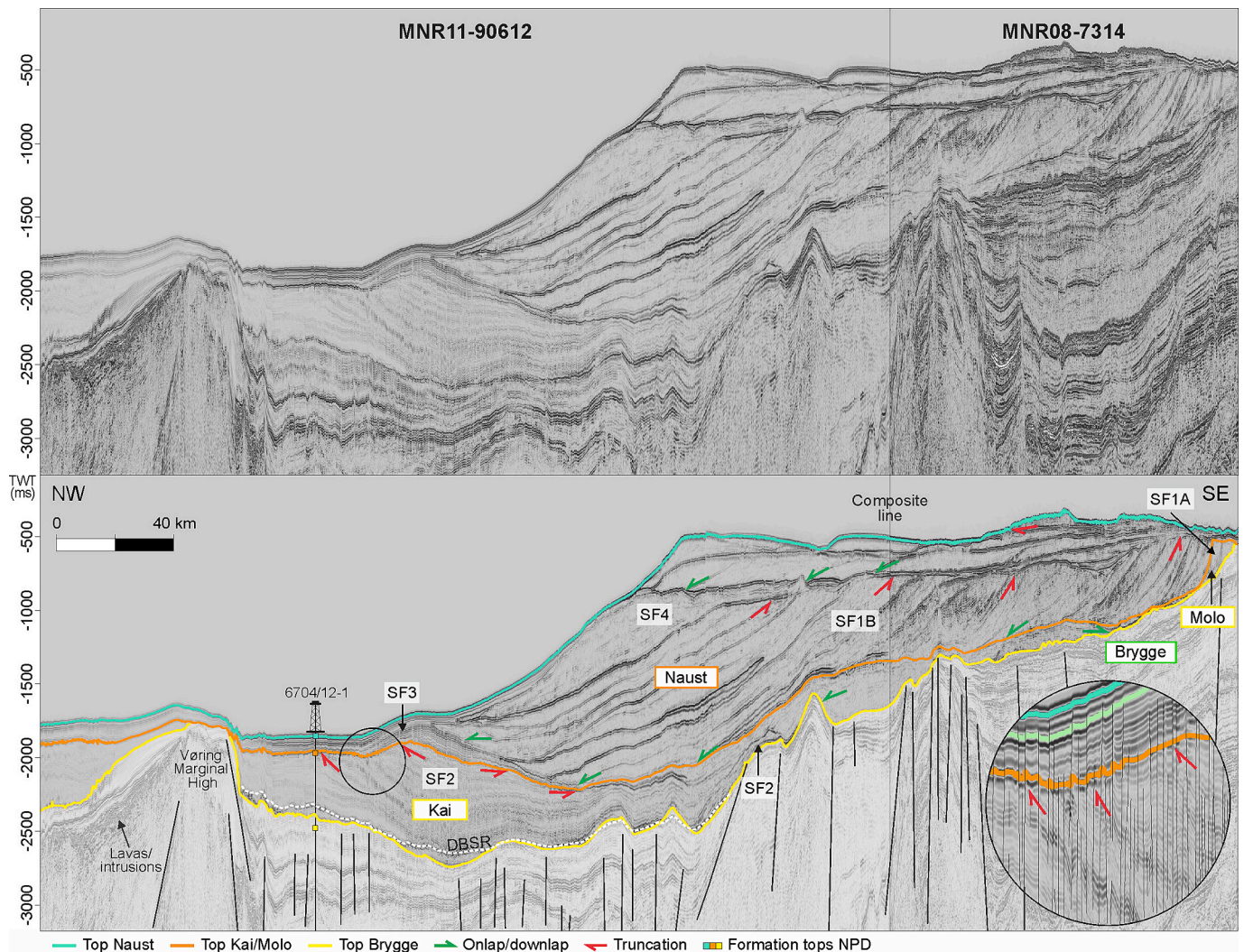


**Fig. 7.** Seismic dip profile crossing the northern mid-Norwegian margin in the area of well 6704/12-1. A diagenetic bottom simulating reflector crosscuts the stratigraphy and the top Brygge horizon. Notice the mismatch between the interpreted top Brygge horizon and the formation pick in well. The top Brygge pick from NPD is most likely incorrect (downloaded from <http://factpage.npd.no>), as it does not correlate with corresponding picks in nearby wells. Inset: Truncation and polygonal faulting of Kai Formation in Vøring Basin. See Fig. 2b for location.

slightly younger deposits (c. 9.6 Ma) upslope and in the east (Fig. 12a) (Eidvin et al., 2007). Based on these ages, and the observed upslope migration of the drifts, we suggest that they began to build up in the basin and on the lower slope. In the distal Vøring Basin, thick deep-water drift systems (IV–VII, Table 3) also developed under the influence of ocean currents, interlayered by hemipelagic to pelagic deposits that formed under near-still conditions (Figs. 7, 11a). Moats and onlap terminations of these systems, along the western flank of the mid-Norwegian domes, indicate that the principal flow was focused here, and that the domes influenced paleocurrents (Fig. 6). The youngest and shallowest drift (I, Table 3), developed close to the foot of Molo Formation on the shelf, implying that ocean currents were active near the coast off mid-Norway since 9.6 Ma (Fig. 11a).

In contrast to previously described drifts, the Kai Formation drifts in the northern mid-Norwegian region accumulated onto a complex relief of highs, ridges and domes. Existing classification systems are therefore not accurately descriptive, c.f., Rebesco and Stow (2001), Faugères and Stow (2008) and Rebesco et al. (2014). Hence, we suggest a new class of drift type named *structurally-controlled drifts*.

The ocean currents in the northern mid-Norwegian region continued northwards in the Miocene, as evidenced by two drifts in the Lofoten–Vesterålen region (VIII–IX, Table 3 and Fig. 8). These drifts are

classified as giant elongated, separated drifts (Faugères and Stow, 2008) with moats along their eastern flank. The drifts developed in a different physiographic setting than the mid-Norwegian drifts, as they onlap onto a steep slope incised by gorges interpreted to be canyons, and onto a basin edge dominated by a fault system (Figs. 10a, 12a, b). As a response to this physiographic setting and more restricted sediment availability, the Lofoten–Vesterålen drifts are less widespread (Figs. 2a, 11a).

Our results show more widespread contourites within the Kai Formation than previously documented, with drifts covering both the paleo-slope and deep basins (Figs. 11a, 12a). The drifts deposited from these currents were likely a response to the North Atlantic–Arctic Ocean connection, which formed due to opening of Fram Strait at ~17 Ma and subsidence of Greenland–Scotland Ridge at ~12 Ma (Wright, 1998; Jakobsson et al., 2007). The fact that subsidence of the ridge occurred nearly synchronous with onset of drift growth, slightly before 11 Ma, indicates free passage of warm North Atlantic Water across the ridge and northwards. A similar expansion of drift growth in the Miocene is recorded all along the Atlantic (e.g., Wold, 1994; Nielsen et al., 2011; Hernández-Molina et al., 2016), the Barents Sea/Fram Strait area (e.g., Eiken and Hinz, 1993; Geissler et al., 2011; Gebhardt et al., 2014; Lasubuda et al., 2018) and in the Arctic Ocean (e.g., Weigelt et al., 2020; Mosher and Boggild, 2021).



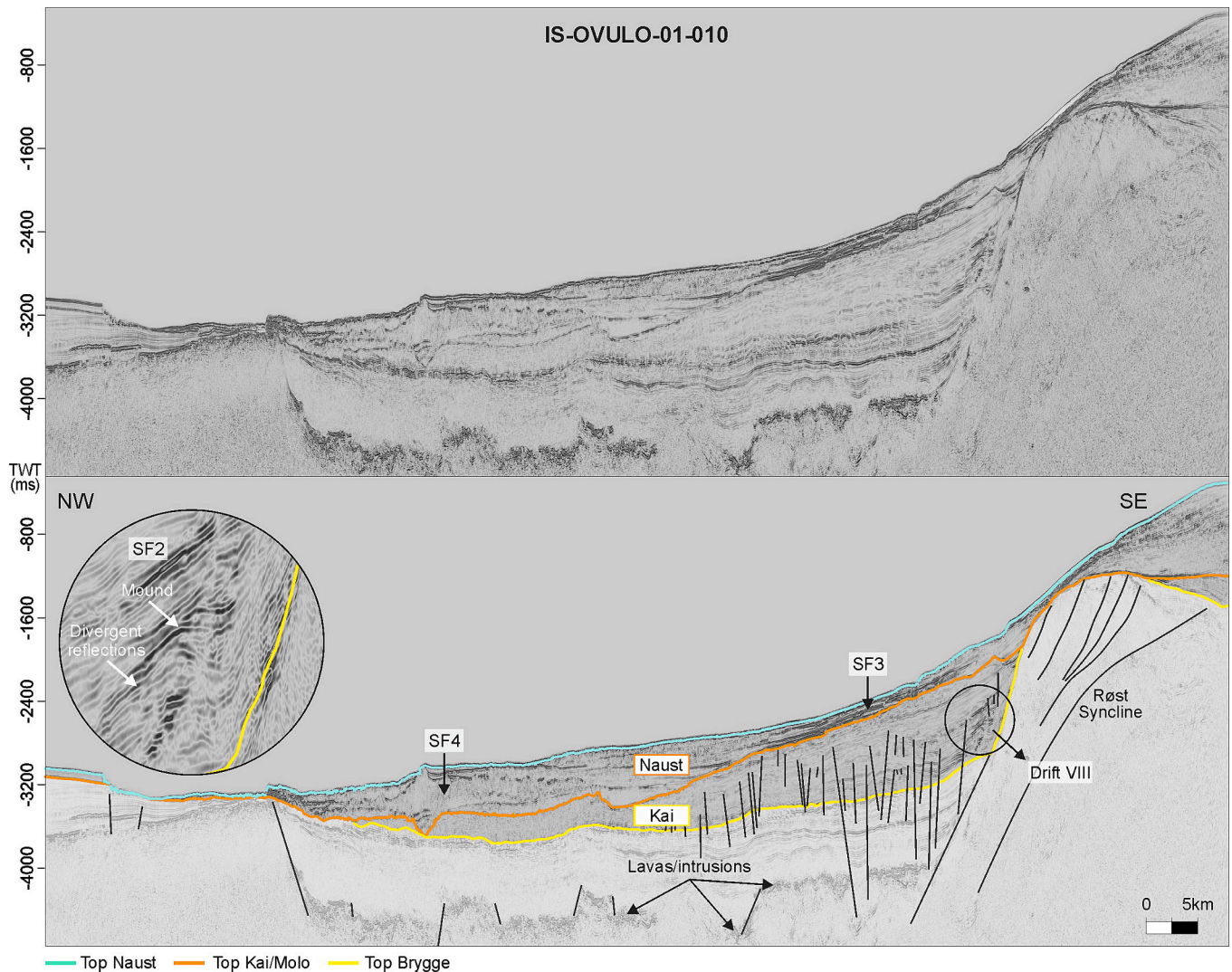


Fig. 8. Seismic dip profile across southern Lofoten Basin. Kai Formation is characterized by polygonal faults and SF2 near the Røst Syncline. SF4 characterizes the Naust Formation in the area of the Trænadjupet Slide. See Fig. 2b for location.

The extensive contourites of the Kai Formation across the northern mid-Norwegian region (I–VII) point to a dominantly alongslope sedimentation, with little influence of downslope processes in the mid-Miocene (Figs. 11a, 12a). Similar conditions are documented on the SW Barents Sea margin during the same period, where the Bjørnøyrenna Drift accumulated (Rydningen et al., 2020). In the steeper Lofoten–Vesterålen region, alongslope sedimentation (VIII and IX) was likely accompanied by focused downslope transport of sediments through canyons on the slope and into Lofoten Basin. Canyon formation is inferred to be a result of uplift that reduced incidents of slope stability (Table 2 and Figs. 10b, 11a) (Rise et al., 2013). Alternatively, this downslope activity may have been a consequence of slope failure in weak contouritic sediments, which began to accumulate within the canyons from this time onwards. Rydningen et al. (2016) linked the steep canyonized slope on the Troms margin, just north of Lofoten–Vesterålen, to an uplift event at the Paleocene–Eocene transition described by Osmundsen and Redfield (2011). Thus, the steep slope has perhaps had a long-term influence on the sedimentation on the Lofoten–Vesterålen–Troms margin, where it probably promoted high flow velocities and caused slumps on the upper slope to transform into debris flows and turbidity currents downslope. The Kai Formation is thin or absent on the steepest parts of the slope in between the canyons, which indicates that the slope, at least partly, acted as a sediment bypass zone

(Fig. 10b).

The SW–NE contour current direction suggests that the main source area for the Kai drifts was somewhere south of the mapped area. It is also likely that some of the sediments initially came from the mainland in the east before subsequently being redeposited northwards by contour currents, i.e., via run-off from the Scandes Mountains.

#### 5.2.2. Late Miocene to Pliocene (~8.8/8.7 Ma to ~2.7 Ma)

The Molo Formation lies on top of the Brygge horizon on the inner northern mid-Norwegian shelf, where it is interpreted to form a deltaic coastal progradational wedge; earlier suggested to have developed due to eustatic sea-level fall and uplift (e.g., Rokoengen et al., 1995; Henriksen and Vorren, 1996; Eidvin et al., 2007, 2019). Seismic mapping in this study reveals that the Molo Formation extends downslope and interfingers with the upper part of the Kai Formation in the central Trænadjupet area, suggesting concurrent deposition for the two formations (Figs. 2a, 5a). Age constraints from exploration wells also support contemporaneous deposition, as the Molo Formation started accumulating in the late Miocene c. 8.8–8.7 Ma (well 6610/3–1) (Grøsfjeld et al., 2019), and ages of c. 6.9 to 5.1 Ma are found for the eastern part of Kai Formation (well 6607/5–1) (Eidvin et al., 2007) (Fig. 12a). Our findings, based on regional seismic mapping differ from the results of Løseth and Henriksen (2005), Løseth et al. (2017) and Løseth (2021),



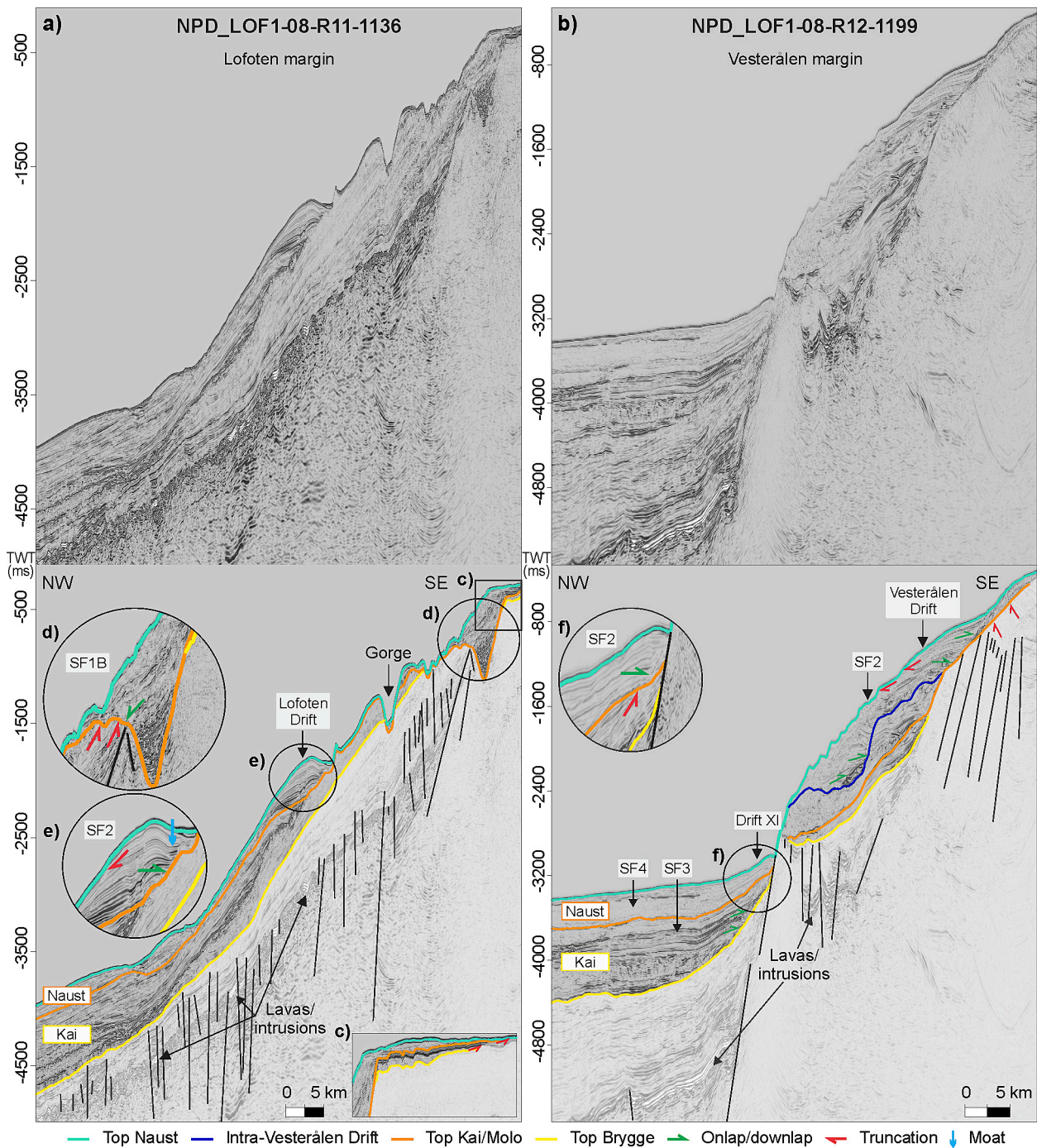


**Fig. 9.** a–b) Seismic dip profile across the slope and basin off Lofoten–Vesterålen. c) Top Brygge and top Kai/Molo horizons are truncated on the Lofoten shelf. d–e) SFB1 fills in a gorge on the upper Lofoten slope, while SF2 dominates downslope. f) SF2 dominates both on the slope and in the basin areas off Vesterålen. See Fig. 2b for location.

who suggest that the formation is of Pliocene age.

The vast extent of the Molo Formation along the coast and its E-W progradational style suggest that it developed due to increased run-off from a wide onshore drainage area in the east, likely the Scandes Mountains (Figs. 10b, 12a). The considerable size of the system also suggests that it formed by several merging deltas, possibly under the influence of ocean currents that redistributed sandy sediments along the margin (Fig. 12a). Based on the location of the thickest part of the formation in the central Trænadjupet Trough, representing the continuation of Vestfjorden to the shelf break, we infer that most of the sediments originated in the Vestfjorden region (Figs. 10, 11a). This interpretation

is consistent with Grøsfjeld et al. (2019), who suggested that the northern Molo Formation was sourced from the Vestfjorden area, with the Vestfjorden lineament serving as a corridor for sediment delivery.

The seaward progradation of the Molo Formation did most likely not commence fully until 8.8–8.7 Ma ago (Grøsfjeld et al., 2019). The construction formed during a period of climatic cooling, following the mid-Miocene Climatic Optimum from 17 to 15 Ma (Zachos et al., 2001). This is a considerably delayed response time after the climatic optimum, implying that it took >6 Ma before the effect of increased humid conditions led to increased onshore erosion from higher rainfall. As an alternative to this delayed climatic response, we speculate that land



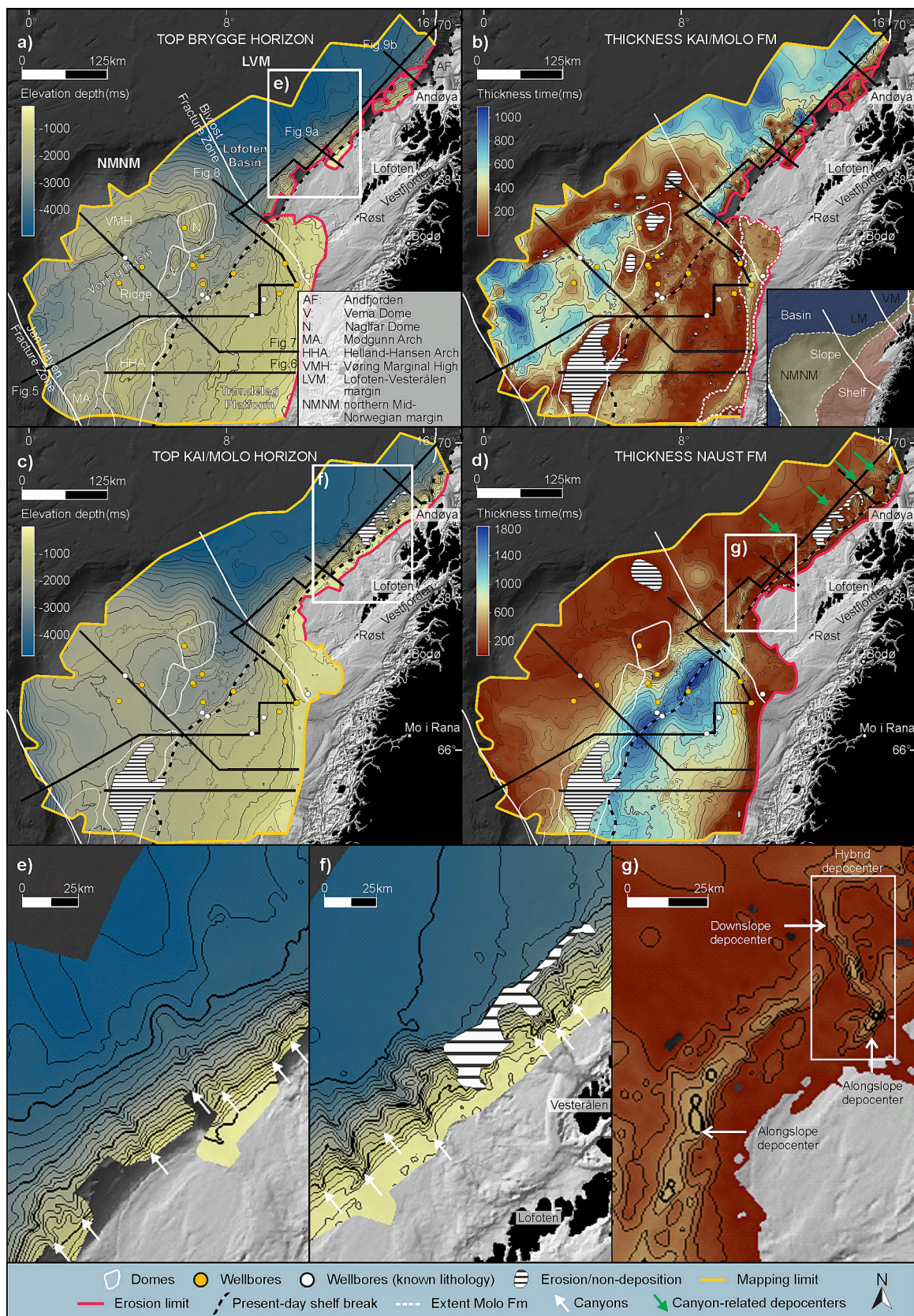


**Fig. 10.** a) and c) Time-structure maps in TWT ms of top Brygge and top Kai/Molo horizons with 200 m contour intervals. b) and d) Isochrone maps of the Kai/Molo and Naust formations with 100 m contour intervals. e) and f) Canyons characterizing the top Brygge and top Kai/Molo horizons off Lofoten–Vesterålen. Canyons are more deeply incised on the top Kai/Molo horizon. g) Along- and downslope depocenters off Lofoten–Vesterålen, belonging to the Naust Formation.

**Table 2**

Summary of seismic horizons and units mapped on the northern mid-Norwegian margin (NMNM) and Lofoten–Vesterålen margin (LVM).

	Area	Characteristics	Interpretation
Naust Fm	LVM	<ul style="list-style-type: none"> <li>■ Mounded accumulations characterized by SF2 (contorted)</li> <li>■ Up to c. 770 ms TWT thick on the slope, while c. 490 ms TWT thick in the basin</li> </ul>	Contourites. Few signs of margin progradation due to the alpine mountains acting as a barrier.
	NMNM	<ul style="list-style-type: none"> <li>■ Wedge-shaped deposits dominated by SF1B (tangential oblique). Intervals of SF4 (chaotic) and SF2 (contorted) occur</li> <li>■ Up to c. 1800 ms TWT thick along the modern shelf break, while it only reaches c. 450 ms TWT in the basins</li> </ul>	Glacial progradational wedge influenced by contourite and slide deposits.
Top Kai/ Molo horizon	LVM	<ul style="list-style-type: none"> <li>■ Steeply dipping surface with deeply incised canyons (slope)</li> <li>■ Deeper and gently sloping area (abyssal plain)</li> </ul>	The relief is a result of deposition of the underlying Kai Formation. No sign of tectonic influence.
	NMNM	<ul style="list-style-type: none"> <li>■ Gently dipping surface that shallows in the modern shelf setting (slope)</li> <li>■ Two large paleo-basins separated by a ridge-form</li> </ul>	Relief formed by deposition of Kai/Molo formations with few evidence of tectonic influence.
Molo Fm	LVM	<ul style="list-style-type: none"> <li>■ Not present.</li> </ul>	May be due to the alpine Lofoten–Vesterålen mountains, preventing large fluvial systems from reaching the margin.
	NMNM	<ul style="list-style-type: none"> <li>■ Wedge-shaped accumulation characterized by steeply inclined reflections of SF1A (tangential oblique).</li> </ul>	Coastal shelf construction from run-off/fluvial systems.
Kai Fm	LVM	<ul style="list-style-type: none"> <li>■ Not present in the shelf setting</li> <li>■ Along- and downslope accumulations dominated by SF2 (contorted) and SF4 (chaotic)</li> <li>■ Up to c. 1050 ms TWT thick on the slope and c. 950 ms TWT in the basin.</li> </ul>	Contourite and mass transport deposits.
	NMNM	<ul style="list-style-type: none"> <li>■ Mound-shaped elongated accumulations consisting of SF2 (contorted)</li> <li>■ c. 450 ms TWT thick on the paleo-slope and c. 1065 ms TWT in the basin.</li> </ul>	Contourites.
Top Brygge horizon	LVM	<ul style="list-style-type: none"> <li>■ Steeply dipping surface incised by canyons (slope).</li> <li>■ Deeper and gently sloping area (abyssal plain).</li> </ul>	Faults influencing the top Brygge relief indicate that it has undergone tectonic activity.
	NMNM	<ul style="list-style-type: none"> <li>■ Gently dipping surface (slope)</li> <li>■ Paleo-basins with ridges, arcs, and domes.</li> </ul>	Faults and structural highs indicate tectonic influences on the evolution of the top Brygge relief.

**Table 3**

Classification and dimensions of alongslope accumulations within Kai and Naust formations. Lengths, widths and thicknesses are maximum values. Accumulations with Roman numerals (I–XI) have been described for the first time in this study. Sklinnadjupet, Nyk, Lofoten and Vesterålen drifts have been described earlier (Laberg et al., 1999, 2001) but the dimensions and thicknesses are from this study.

Formation	Area	Alongslope accumulation	Length (km)	Width (km)	Thickness (ms TWT)
Kai Fm	NMNM	I	160	45	400
		II	95	40	225
		III	280	110	455
		IV	150	70	720
		V	70	40	780
		VI	85	75	865
		VII	70	40	960
		VIII	70	55	930
		IX	125	25	500
		X	185	150	785
Naust Fm	NMNM	Sklinnadjupet Drift	85	70	450
		Nyk Drift	75	35	265
		XI	65	10	225
		Lofoten Drift	110	35	575
		Vesterålen Drift	65	30	770



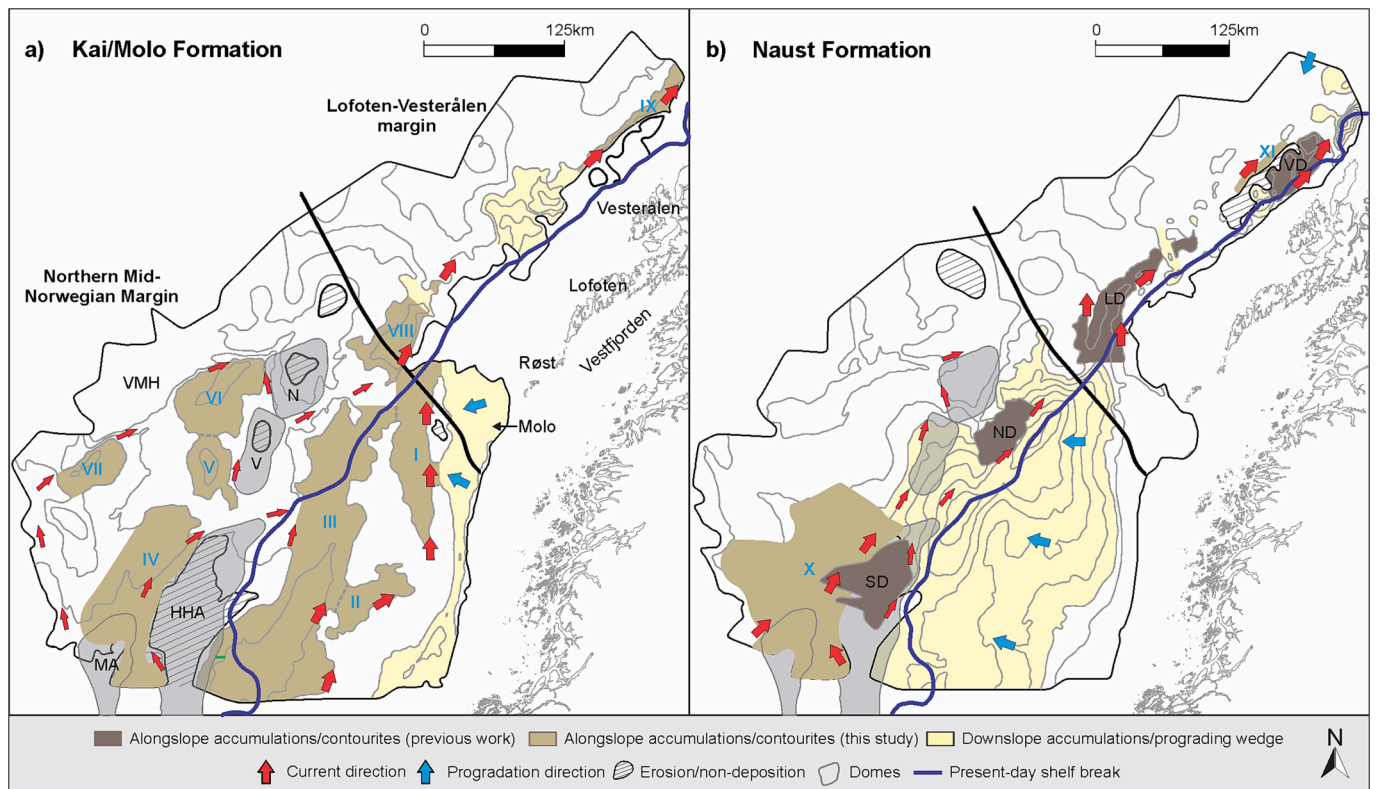


**Fig. 11.** Geographic distribution of along- and downslope accumulations. Contours are from isochrone maps b) and d) in Fig. 10. HHA – Helland-Hansen Arch; LD – Lofoten Drift; MA – Modgunn Arch; N – Naglfar Dome; ND – Nyk Drift; SD – Sklinnadjupet Drift; V – Vema Dome; VD – Vesterålen Drift; VMH – Vøring Marginal High.

uplift instead facilitated increased erosion of the hinterland and thus allowed for westward transport of sediment. Several phases of Cenozoic uplift of the Scandes have been identified (Riis and Fjeldskaar, 1992; Riis, 1996; Lidmar-Bergström et al., 2007, 2013), and these might explain increased sedimentation in the basin areas (Gołdowski et al., 2012; Pedersen et al., 2018). As such, this explanation is preferred over the ICE hypothesis, which would have required an improbable long delay in erosion due to increased rainfall following the climatic optimum.

Coastal progradation from run-off through fluvial systems was far less developed in the Lofoten–Vesterålen region. Alpine mountains probably existed here during the Miocene, and these may have, at least partly, formed from Paleogene rift-flank uplift (Lasabuda et al., 2021). The mountains possibly acted as a barrier that prevented larger fluvial systems from reaching the coast and shelf. Instead, local rivers from smaller drainage areas such as V-shaped valleys perhaps acted as transport agents to the canyons. Absence of Molo Formation in the Lofoten–Vesterålen region could also be attributed to the nature of the underlying top Brygge relief. The wide and low-angle relief off mid-Norway at the time was probably well suited for hosting sediments. Such margins often develop from a low-alpine hinterland morphology (e.g., Sømme et al., 2009), which was probably the case for the mid-Norway hinterland in the late Miocene to Pliocene.

### 5.2.3. Early Quaternary and Holocene (~2.7 to present-day)

Earlier studies (e.g., Rise et al., 2005; Ottesen et al., 2009; Montelli et al., 2017) have described the Naust Formation off mid-Norway as a glacial wedge showing morphologies from past glacial processes, partly subjected to downslope remobilization. The wedge also comprises previously described hemipelagic and contouritic deposits such as the Nyk and Sklinnadjupet drifts (Fig. 6). West of the Helland-Hansen Arch, a well-developed contourite drift (X) dominates the Naust Formation. This drift is classified as a giant elongated drift after Faugères and Stow

(2008), and its presence indicates that contour currents controlled the sediment transport and deposition in the distal margin areas (Fig. 11b). This interpretation coincides with the iceberg drift pattern on the mid-Norwegian margin, revealing that a persistent ocean circulation with NE-flowing currents existed here through the Quaternary (Montelli et al., 2018; Newton et al., 2018). Contourites also represent a significant part of lower Quaternary sediments in the northern North Sea Basin, south of the study area (Batchelor et al., 2017). The fact that Drift X lies directly on top of contouritic deposits within the older Kai Formation (IV), suggests that these currents were active, without significant disruption, from mid-Miocene.

The cause of the abrupt decrease in sediment thickness of the Naust Formation across the Bivrost Lineament is uncertain, but it may be related to late tectonic activity and uplift of the Lofoten–Vesterålen region, where this lineament played an important role (Fig. 10d). The absence of a major glacial progradational wedge in the Lofoten–Vesterålen region is likely related to the continued presence of onshore alpine mountains that reduced delivery of glacial sediments to the adjacent margin and basin (Ottesen et al., 2005). However, three significantly smaller glacial progradational systems fill in canyons on the upper Lofoten–Vesterålen slope beyond the trough mouths (Figs. 9a, 11b). These systems probably formed due to glacial drainage from local ice caps. The bank-trough configuration in the modern shelf setting (Fig. 2b), as well as the moraines, grounding zone wedges and glacial lineations identified by Vorren et al. (2015) support a glacial environment. The seafloor morphology reveals a direct connection between cross-shelf troughs and the head of canyons on the slope. This connection suggests that paleo-ice streams from the ice caps had their outlet at the head of these canyons, which resulted in delivery of subglacial sediments directly into the canyons, where they later remobilized downslope as debris flows and turbidity currents, ending up in the Lofoten Basin (Figs. 2b, 10d).

Downslope of the glacial progradational systems, the previously

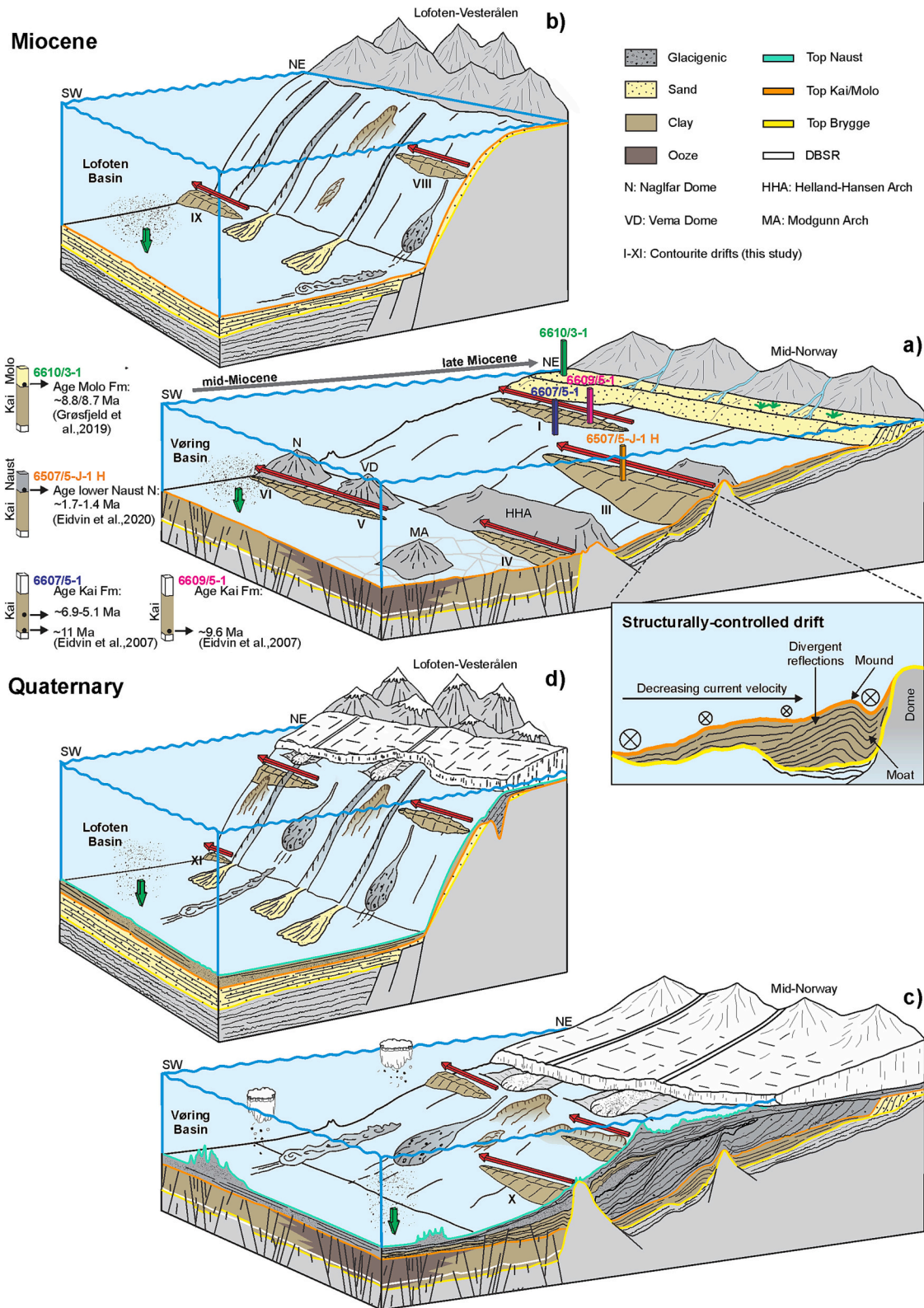


**Fig. 12.** The Miocene–Quaternary evolution of the mid-Norwegian and Lofoten–Vesterålen regions. a) Ocean currents dominated the Vøring Basin and the slope in the mid-Miocene, while slope aggradation occurred on the shelf in the late Miocene. b) Mass-transport processes and ocean currents dominated on the steep Lofoten–Vesterålen slope during the Miocene, whereas ocean currents operated in the Lofoten Basin. c) Build-up of onshore ice sheets increased the sediment supply on the mid-Norwegian margin and formed a large glacigenic progradational wedge. d) On the Lofoten–Vesterålen margin, the sediment input from land was low because alpine mountains blocked the major ice drainage to reach the margin. Instead, contour currents prevailed at the time, building up drifts on the slope. DBSR – Diagenetic bottom simulating reflector.



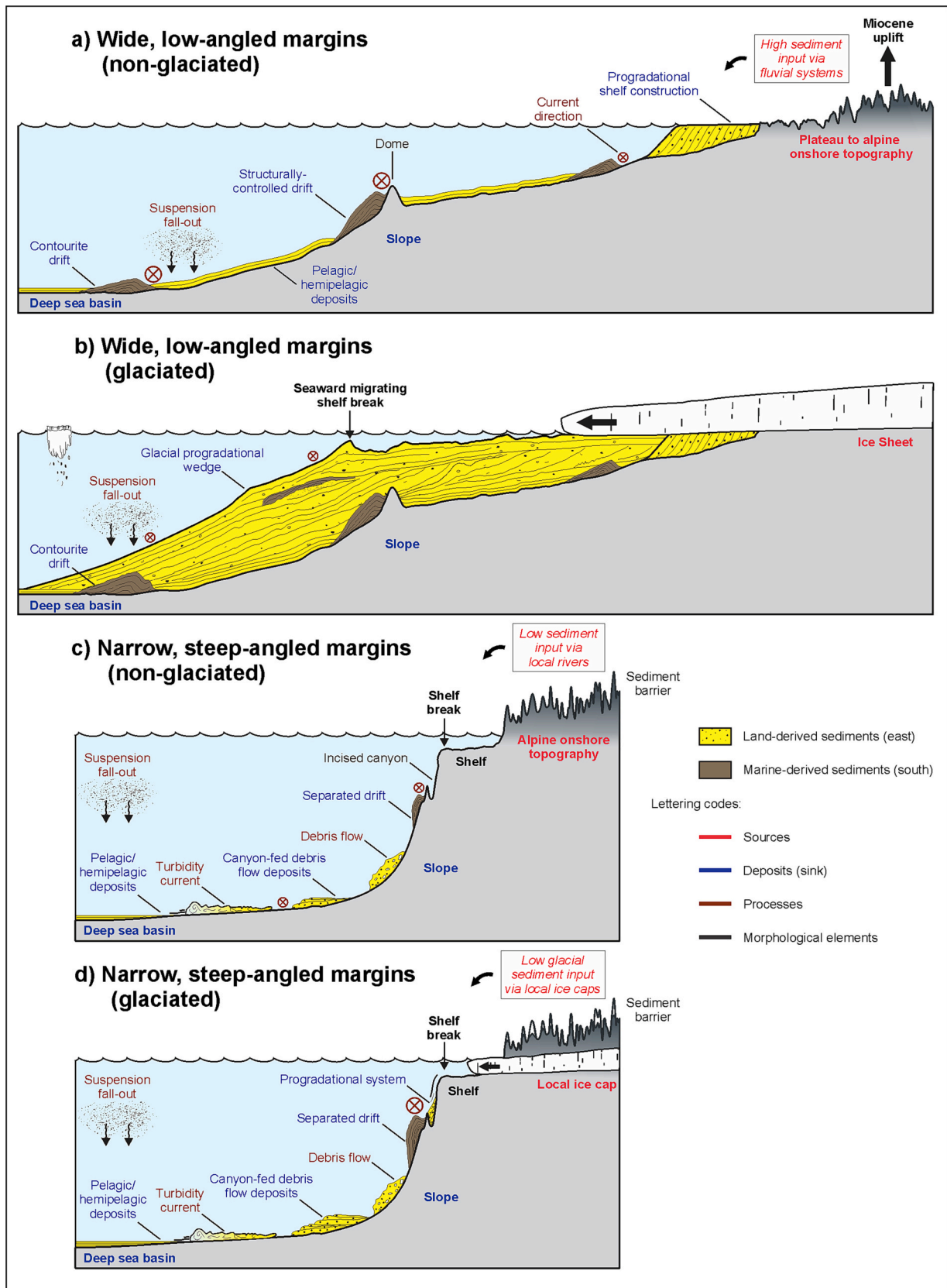


**Fig. 13.** Conceptual model of sedimentary processes and their related deposits on wide low-angled passive margins (a and b) versus narrow steep-angled passive margins (c and d) during non-glacial and glacial conditions. The size of the current direction symbols correlates to the relative current strength, i.e., the larger the symbol the stronger the current.

described Lofoten and Vesterålen drifts (Laberg et al., 1999, 2001) are situated between zones of mass-transport deposits and sediment bypass (Table 2). Our mapping shows that both drifts overlie the top Kai/Molo horizon, which implies that they started to accumulate as late as early Quaternary and not in the mid-Miocene, as previously suggested by Laberg et al. (2001). Intervals of mass-transport deposits occur throughout both drift bodies, indicating that mass wasting processes also affected drift evolution.

The Lofoten Basin is dominated by mass-transport deposits in continuation of the largest canyons on the slope, implying that these were active transport systems during the Quaternary (Figs. 2a, 10d). The largest accumulation occurs beyond the outlet of Andøya Canyon near Andfjorden, suggesting that this system was one of the most efficient transport routes from the slope to basin (Fig. 10d). This efficiency was likely related to high sediment input from paleo-ice streams along Andfjorden Trough on the adjacent shelf (Amundsen et al., 2015), as this trough acted as one of the main pathways for fluvial and glacial drainage systems from central Fennoscandia (Vorren and Plassen, 2002; Ottesen et al., 2005; Rise et al., 2013; Rydningen et al., 2013, 2016). Glacimarine sediments are also present in the Lofoten Basin together with an elongated separated drift (XI) that is confined to the basin flank off Vesterålen. This drift demonstrates that there was deep-water transport of sediments also in this area, similar to the drift in the deeper areas of the mid-Norwegian region (drift X) (Fig. 11b).

The E-W progradational style of the mid-Norwegian Naust wedge, and its maximum thickness near the outlet of Vestfjorden indicates that the Scandes Mountains in the east were the main sediment source (Fig. 11b). A similar through-canyon transport path for the smaller progradational systems in the Lofoten–Vesterålen region points to the alpine Scandes Mountains as the likely source area also for these sediments (Fig. 11b). The northernmost depocenter in the Lofoten Basin prograded from north to south, indicating that these sediments were sourced from the north, and represent parts of the Bear Island TMF that prograded into the abyssal plain of the Lofoten Basin (Figs. 10d, 11b) (Vorren and Laberg, 1997; Laberg et al., 2018).

The SW-NE orientation of the contourites along both margin segments implies a source area to the south. Substantial intensification of drift deposition in the Lofoten–Vesterålen region during the Quaternary compared to the Miocene and Pliocene was probably related to the glacial margin progradation in the mid-Norwegian region. This build out presumably provided source material available for redistribution northwards to the Lofoten–Vesterålen area via ocean currents.

### 5.3. Source-to-sink models on glaciated continental margins

The study area shows similarities with morphological characteristics of source-to-sink systems proposed by Sømme et al. (2009), Helland-Hansen et al. (2016) and Nyberg et al. (2018b). The mid-Norwegian region is comparable with “wide and deep” systems that have small mountainous source areas, wide and low-gradient shelves, few or no canyons on the slope, and deep basins (Figs. 13a, b) (Helland-Hansen et al., 2016; Nyberg et al., 2018a, 2018b). The Lofoten–Vesterålen region has a similar morphology as “steep, short, and deep” systems that exhibit steep gradients a prominent onshore topography, narrow shelves, deep basins and a sediment transport to the deep-marine realm through submarine canyons (Figs. 13c, d) (Helland-Hansen et al., 2016; Nyberg et al., 2018b).

The relative importance of along- and downslope processes in the study area was likely controlled by topographic variations along the onshore hinterland and margin, as well as by global climate (glacial and non-glacial). The main sediment input was from the mainland in the east and the marine environment in the south, of which sediments were brought to and redistributed from the margin and deep basins by different processes (Figs. 12, 13). Fluvial and glacial processes were efficient transport agents for sediments from the mainland, while ocean currents transferred sediments from the south.

Similar shelf progradational glacial wedges, with a low-relief hinterland as on the mid-Norwegian margin are observed on other glaciated margins, such as on the Canadian Atlantic margin (e.g., Piper, 2005), Argentine margin (Gruetzner et al., 2012) and parts of the Antarctic margin (Cooper et al., 1991; Kuvaas and Kristoffersen, 1991; De Santis et al., 1995; Kim et al., 2018; Conte et al., 2021). In contrast, similar types of continental margins as the Lofoten–Vesterålen margin, with an alpine hinterland, narrow shelves and steep slopes generally with less developed TMFs, are also found on parts of the northern Svalbard margin (Lasabuda et al., 2018), on the SE and SW Greenland margin (Clausen, 1998; Rasmussen et al., 2003a; Nielsen et al., 2005; Batchelor and Dowdeswell, 2014) and along the Antarctic Peninsula (Hernández-Molina et al., 2017).

Both margin types in this study and in the examples above from other areas are overlain by the global ocean conveyor belt, where contourites typically accumulate (Fig. 13) (e.g., Faugères et al., 1993; Gilbert et al., 1998; Hernández-Molina et al., 2009; Rodrigues et al., 2021). Ocean currents are therefore an important sediment transport mechanism along such margins of which is often neglected in source-to-sink models. Helland-Hansen et al. (2016), touched upon the influence of alongshore current transport on these systems but it is not fully accounted for in their models. The significant volume of contourites interpreted in this study demonstrates that future work on source-to-sink models should more often consider the role of ocean currents, and thereby the potential for multiple sources to the sink. This interpretation is supported by volume calculations of mostly Cenozoic sediments along other sectors of the Atlantic margin, such as offshore United States and Canada where contourite deposition have been estimated to account for sediment volumes of c. 683,000 km<sup>3</sup>, while submarine fan deposition accounted for a volume of only c. 178,000 km<sup>3</sup> (Mosher and Yanez-Carrizo, 2021).

Our results further show that the underlying relief has influenced the sedimentation pattern of contourites. On wide and gentle margins with structural highs, thick drifts typically fill in bathymetric lows between the highs due to a reduction in current velocities. This antecedent morphologic influence on drift development leads to a new class of contourite drift that we term “structurally-controlled” drifts (Fig. 13a). In contrast, the thin sediment cover between the drifts, i.e., at the structural high crests, reflects areas of erosion where current velocities exceed the threshold for deposition. These velocities may be related to a funneling effect for the ocean currents in these areas. By contrast, narrow and steep margins favor development of giant elongated separated drifts; a drift type that is separated by moats where the principal flow was focused, and where erosion or non-deposition dominated (Figs. 13c, d) (Rebesco et al., 2014).

## 6. Conclusion

The Neogene–Quaternary paleoenvironmental evolution of the northern mid-Norwegian and the Lofoten–Vesterålen margins is deciphered mainly using 2D seismic data and exploration wells. The following conclusions can be made:

1. A total of 11 new contourite drifts, named I–XI, have been defined in the Kai and Naust formations. These drifts are up to 280 km long, 150 km wide and 960 ms TWT thick. Together with previously known drifts from this area (Nyk, Sklinnadjupet, Lofoten and Vesterålen drifts), they represent part of one large drift system related to NE-flowing Atlantic Water through the Neogene and Quaternary. Some drifts accumulated on a complex underlying relief with structural highs, and we therefore propose a new class of drift types, here named *structurally-controlled drifts*.
2. Kai Formation is on the mid-Norwegian margin mostly composed of drifts that commenced in the mid-Miocene (slightly before 11 Ma), while a mix of drifts and mass-transport deposits is interpreted for the Lofoten–Vesterålen margin. The drifts probably developed because of regional ocean circulation in the Norwegian–Greenland



Sea, following opening of Fram Strait (17 Ma) and subsidence of Greenland–Scotland Ridge (12 Ma). Ridge subsidence to the south was likely a key factor, as it occurred almost synchronously with the onset of drift growth.

- Molo Formation initiated on the mid-Norwegian shelf in the late Miocene (8.8 Ma). Coastal progradation of this formation interfingered with drift growth on the slope in Kai Formation, showing contemporaneous deposition of the two formations up until 2.7 Ma.
- The late onset of Molo progradation (8.8 Ma) compared with timing of the mid-Miocene Climatic Optimum (17–15 Ma), favors Miocene uplift over climatic cooling as the initiation mechanism; a mechanism that also supports the “classical” hypothesis concerning the origin of the Scandes.
- Although Naust Formation in the mid-Norwegian region mainly built out as a glacial progradational wedge throughout Quaternary (2.7–0 Ma), its development was also characterized by significant intervals of contourite sedimentation. A similar progradational wedge is less prominent in the Lofoten–Vesterålen region, where downslope sedimentation was canyon-controlled, while ocean currents redistributed sediments from the south and constructed the large Lofoten and Vesterålen drifts in the Quaternary (previously assumed to be of Miocene age).
- The distinct difference in margin construction between the mid-Norwegian and Lofoten–Vesterålen segments is believed to result from hinterland and basin topography. The low-lying hinterland of the mid-Norwegian region allowed for a large fluvial and later glacial source area, where the adjacent broad and low-angled margin facilitated extensive progradational sequences from these. Such progradational sequences are restricted in the narrow and steep Lofoten–Vesterålen region, as the sediments here originated from a small alpine hinterland that were mostly routed through canyons into the deep basins.
- Drift construction occurred in both margin segments throughout the Neogene and Quaternary, where contour currents brought sediments from parts of the margin further south. The widespread drifts demonstrate the importance of ocean currents in source-to-sink systems and underlines the need for ocean currents that both erode and deposit sediments, to be integrated in future source-to-sink models.

#### Declaration of Competing Interest

The authors declare that they have no known competing financial interests or personal relationships that could have appeared to influence the work reported in this paper.

#### Data availability

We thank UiT The Arctic University of Norway for providing seismic lines collected on cruises between 2000 and 2010, as well as TGS for providing the unreleased MNR04-11 seismic data (<http://www.tgs.com>). Furthermore, we are grateful to NPD for providing the public seismic data from the Diskos database (<http://www.npd.no/en/diskos/>), as well as the unpublished NPD-LOF1-07/08 and the NPD-LOF1-09 seismic data. For permission to access the seismic data, please contact these institutions. The seismic data from UiT The Arctic University of Norway are available at UiT’s open research data repository: <https://dataverse.no/dataverse/uit>.

#### Acknowledgements

This study was part of the Research Center for Arctic Petroleum Exploration (ARCEX) project, which was funded by the Research Council of Norway (grant number 228107) together with the ARCEX partners. Lasabuda acknowledges a grant from the Equinor–UiT *Akademia* agreement. The perceptually uniform color maps of Crameri et al.

(2020) were used to prevent visual distortion of the data. We are grateful to Rowan Romeyn and Carmen Avery Braun for proofreading the manuscript and figures. Finally, we thank the Editor and three anonymous reviewers for their detailed and constructive comments that greatly improved the manuscript.

#### References

- Amundsen, H.B., Laberg, J.S., Vorren, T.O., Hafliðason, H., Forwick, M., Buhl-Mortensen, P., 2015. Late Weichselian–Holocene evolution of the high-latitude Andøya submarine Canyon, North-Norwegian continental margin. *Mar. Geol.* 363, 1–14. <https://doi.org/10.1016/j.margeo.2015.02.002>.
- Badley, M.E., 1985. *Practical Seismic Interpretation*. International Human Resources Development Corporation, Boston.
- Baeten, N.J., Laberg, J.S., Forwick, M., Vorren, T.O., Vanneste, M., Forsberg, C.F., et al., 2013. Morphology and origin of smaller-scale mass movements on the continental slope off northern Norway. *Geomorphology* 187, 122–134. <https://doi.org/10.1016/j.geomorph.2013.01.008>.
- Baeten, N.J., Laberg, J.S., Vanneste, M., Forsberg, C.F., Kvalstad, T.J., Forwick, M., et al., 2014. Origin of shallow submarine mass movements and their glide planes—Sedimentological and geotechnical analyses from the continental slope off northern Norway. *J. Geophys. Res. Earth Surf.* 119 (11), 2335–2360. <https://doi.org/10.1002/2013JF003068>.
- Batchelor, C.L., Dowdeswell, J.A., 2014. The physiography of High Arctic cross-shelf troughs. *Quat. Sci. Rev.* 92, 68–96. <https://doi.org/10.1016/j.quascirev.2013.05.025>.
- Batchelor, C.L., Ottesen, D., Dowdeswell, J.A., 2017. Quaternary evolution of the northern North Sea margin through glacial debris-flow and contourite deposition. *J. Quat. Sci.* 32 (3), 416–426. <https://doi.org/10.1002/jqs.2934>.
- Bellwald, B., Batchelor, C., Garcia, A., Barrett, R., Rosenqvist, M., Planke, S., et al., 2022. *Contourites of the Northern North Sea, North Sea Fan, and Mid-Norwegian Margin*. Paper presented at the 83rd EAGE Annual Conference & Exhibition.
- Blystad, P., 1995. Structural elements of the Norwegian continental shelf. Part 2: the Norwegian Sea region. *NPD Bull.* 8.
- Boyle, E.A., Keigwin, L., 1987. North Atlantic thermohaline circulation during the past 20,000 years linked to high-latitude surface temperature. *Nature* 330 (6143), 35–40. <https://doi.org/10.1038/330035a0>.
- Bruns, P., Dullo, W.-C., Hay, W.W., Frank, M., Kubik, P., 1998. Hiatuses on Vøring Plateau: sedimentary gaps or preservation artifacts? *Mar. Geol.* 145 (1–2), 61–84. [https://doi.org/10.1016/S0025-3227\(97\)00111-4](https://doi.org/10.1016/S0025-3227(97)00111-4).
- Bryn, P., Berg, K., Stoker, M., Hafliðason, H., Solheim, A., 2005. Contourites and their relevance for mass wasting along the Mid-Norwegian Margin. *Mar. Pet. Geol.* 22 (1–2), 85–96. <https://doi.org/10.1016/j.marpetgeo.2004.10.012>.
- Buhl-Mortensen, L., Hodnesdal, H., Thorsnes, T., 2010. Til bunns i Barentshavet og havområdene utenfor Lofoten—ny kunnskap fra MAREANO for økosystembasert forvaltning. Geological Survey of Norway, Trondheim.
- Buhl-Mortensen, L., Bøe, R., Dolan, M.F.J., Buhl-Mortensen, P., Thorsnes, T., Elvenes, S., Hodnesdal, H., 2012. Banks, troughs, and canyons on the continental margin off Lofoten, Vesterålen, and Troms, Norway. In: Harris, P.T., Baker, E.K. (Eds.), *Seafloor Geomorphology as Benthic Habitat*. Elsevier, pp. 703–715.
- Bull, S., Cartwright, J., Huuse, M., 2009. A review of kinematic indicators from mass-transport complexes using 3D seismic data. *Mar. Pet. Geol.* 26 (7), 1132–1151. <https://doi.org/10.1016/j.marpetgeo.2008.09.011>.
- Chand, S., Rise, L., Knies, J., Hafliðason, H., Hjelstuen, B.O., Bøe, R., 2011. Stratigraphic development of the south Vøring margin (Mid-Norway) since early Cenozoic time and its influence on subsurface fluid flow. *Mar. Pet. Geol.* 28 (7), 1350–1363. <https://doi.org/10.1016/j.marpetgeo.2011.01.005>.
- Clausen, L., 1998. The Southeast Greenland glaciated margin: 3D stratigraphic architecture of shelf and deep sea. In: Stoker, M., Evans, D., Cramp, A. (Eds.), *Geological Processes on Continental Margins: Sedimentation, Mass-Wasting and Stability*, Vol. 129, pp. 173–203. Geological Society, London, Special Publications.
- Cohen, K.M., Finney, S.C., Gibbard, P.L., Fan, J.-X., 2016. The ICS international chronostratigraphic chart. *Episodes* 36 (3), 199–204.
- Conte, R., Rebesco, M., De Santis, L., Colleoni, F., Bensi, M., Bergamasco, A., et al., 2021. Bottom current control on sediment deposition between the Iselin Bank and the Hillary Canyon (Antarctica) since the late Miocene: an integrated seismic-oceanographic approach. *Deep-Sea Res. I Oceanogr. Res. Pap.* 176, 103606 <https://doi.org/10.1016/j.dsr.2021.103606>.
- Cooper, A.K., Barrett, P.J., Hinz, K., Traube, V., Letichenkov, G., Stagg, H.M.J., 1991. Cenozoic prograding sequences of the Antarctic continental margin: a record of glacio-eustatic and tectonic events. *Mar. Geol.* 102 (1–4), 175–213. [https://doi.org/10.1016/0025-3227\(91\)90008-R](https://doi.org/10.1016/0025-3227(91)90008-R).
- Corner, G.D., 2005. Scandes mountains. In: Seppälä, M. (Ed.), *The Physical Geography of Fennoscandia*. Oxford University Press, Oxford, pp. 229–254.
- Crameri, F., Shephard, G.E., Heron, P.J., 2020. The misuse of colour in science communication. *Nat. Commun.* 11 (1), 1–10. <https://doi.org/10.1038/s41467-020-19160-7>.
- Dahlgren, K.T., Vorren, T.O., Laberg, J.S., 2002. Late Quaternary glacial development of the mid-Norwegian margin—65 to 68°N. *Mar. Pet. Geol.* 19 (9), 1089–1113. [https://doi.org/10.1016/S0264-8172\(03\)00004-7](https://doi.org/10.1016/S0264-8172(03)00004-7).
- Dahlgren, K.I.T., Vorren, T.O., Stoker, M.S., Nielsen, T., Nygård, A., Sejrup, H.P., 2005. Late Cenozoic prograding wedges on the NW European continental margin: their formation and relationship to tectonics and climate. *Mar. Pet. Geol.* 22 (9–10), 1089–1110. <https://doi.org/10.1016/j.marpetgeo.2004.12.008>.

- de Castro, S., Miramontes, E., Dorador, J., Jouet, G., Cattaneo, A., Rodríguez-Tovar, F.J., Hernández-Molina, F.J., 2021. Siliciclastic and bioclastic contouritic sands: Textural and geochemical characterisation. *Mar. Pet. Geol.* 128, 105002 <https://doi.org/10.1016/j.marpetgeo.2021.105002>.
- De Santis, L., Anderson, J.B., Brancolini, G., Zayatz, I., 1995. Seismic record of late Oligocene through Miocene glaciation on the central and eastern continental shelf of the Ross Sea. In: Cooper, A.K., Barker, P.F., Brancolini, G. (Eds.), *Geology and Seismic Stratigraphy of the Antarctic Margin*, Vol. 68, pp. 235–260.
- Dehls, J.F., Olesen, O., Bungum, H., Hicks, E.C., Lindholm, C.D., Riis, F., 2000. Neotectonic Map: Norway and Adjacent Areas. Geological Survey of Norway.
- Dowdeswell, J.A., Ottesen, D., Rise, L., 2010. Rates of sediment delivery from the Fennoscandian Ice Sheet through an ice age. *Geology* 38 (1), 3–6. <https://doi.org/10.1130/G25523.1>.
- Dybkiær, K., Rasmussen, E.S., Eidvin, T., Grøsfjeld, K., Riis, F., Piasecki, S., Śliwińska, K., 2020. A new stratigraphic framework for the Miocene–Lower Pliocene deposits offshore Scandinavia: a multiscale approach. *Geol. J.* 56 (3), 1699–1725. <https://doi.org/10.1002/gj.3982>.
- Ehlers, B.-M., Jokat, W., 2013. Paleo-bathymetry of the northern North Atlantic and consequences for the opening of the Fram Strait. *Mar. Geophys. Res.* 34 (1), 25–43. <https://doi.org/10.1007/s11001-013-9165-9>.
- Eidvin, T., Bugge, T., Smelror, M., 2007. The Molo Formation, deposited by coastal progradation on the inner Mid-Norwegian continental shelf, coeval with the Kai Formation to the west and the Utsira Formation in the North Sea. *Nor. J. Geol.* 87, 75–142.
- Eidvin, T., Riis, F., Rasmussen, E.S., 2014. Oligocene to Lower Pliocene deposits of the Norwegian continental shelf, Norwegian Sea, Svalbard, Denmark and their relation to the uplift of Fennoscandia: A synthesis. *Mar. Pet. Geol.* 56, 184–221. <https://doi.org/10.1016/j.marpetgeo.2014.04.006>.
- Eidvin, T., Rasmussen, E.S., Riis, F., Dybkiær, K., Grøsfjeld, K., 2019. Correlation of the Upper Oligocene–Miocene deltaic to shelfal succession onshore Denmark with similar deposits in the northern North Sea and Norwegian Sea shelf based on Sr isotope-, bio- and seismic stratigraphy - a review. *Nor. J. Geol.* 99 (4), 543–573. <https://doi.org/10.17850/njg99-4-1>.
- Eidvin, T., Ottesen, D., Dybkiær, K., Rasmussen, E.S., Riis, F., 2020. The use of Sr isotope stratigraphy to date the Pleistocene sediments of the Norwegian continental shelf - a review. *Nor. J. Geol.* 100 (1), 1–35.
- Eidvin, T., Riis, F., Brekke, H., Smelror, M., 2022. A revised lithostratigraphic scheme for the Eocene to Pleistocene succession on the Norwegian continental shelf. *Norwegian J. Geol. Special Publication 1*. <https://doi.org/10.17850/njgsp1, 1-XXX>.
- Eiken, O., Hinz, K., 1993. Contourites in the Fram Strait. *Sediment. Geol.* 82 (1–4), 15–32. [https://doi.org/10.1016/0037-0738\(93\)90110-Q](https://doi.org/10.1016/0037-0738(93)90110-Q).
- Eidevik, T., Nilsen, J.E.Ø., 2013. The Arctic–Atlantic thermohaline circulation. *J. Clim.* 26 (21), 8698–8705. <https://doi.org/10.1175/JCLI-D-13-00305.1>.
- Eldholm, O., Faleide, J.I., Myhre, A.M., 1987. Continent-ocean transition at the western Barents Sea/Svalbard continental margin. *Geology* 15 (12), 1118–1122. [https://doi.org/10.1130/0091-7613\(1987\)15<1118:CTATWB>2.0.CO;2](https://doi.org/10.1130/0091-7613(1987)15<1118:CTATWB>2.0.CO;2).
- Evans, D., Harrison, Z., Shannon, P.M., Laberg, J.S., Nielsen, T., Ayers, S., et al., 2005. Palaeoslides and other mass failures of Pliocene to Pleistocene age along the Atlantic continental margin of NW Europe. *Mar. Pet. Geol.* 22 (9–10), 1131–1148. <https://doi.org/10.1016/j.marpetgeo.2005.01.010>.
- Faleide, J.I., Tsikalas, F., Breivik, A.J., Mjelde, R., Ritzmann, O., Engen, O., et al., 2008. Structure and evolution of the continental margin off Norway and the Barents Sea. *Episodes* 31 (1), 82–91. <https://doi.org/10.18814/epiugs/2008/v31i1/012>.
- Faugères, J.-C., Stow, D.A.V., 2008. Contourite drifts: nature, evolution and controls. In: *Rebesco, M., Camerlenghi, A. (Eds.), Developments in Sedimentology*, vol. 60. Elsevier, Amsterdam, pp. 257–288.
- Faugères, J.-C., Mézerais, M.L., Stow, D.A.V., 1993. Contourite drift types and their distribution in the North and South Atlantic Ocean basins. *Sediment. Geol.* 82 (1–4), 189–203. [https://doi.org/10.1016/0037-0738\(93\)90121-K](https://doi.org/10.1016/0037-0738(93)90121-K).
- Faugères, J.-C., Stow, D.A.V., Imbert, P., Viana, A., 1999. Seismic features diagnostic of contourite drifts. *Mar. Geol.* 162 (1), 1–38. [https://doi.org/10.1016/S0025-3227\(99\)00068-7](https://doi.org/10.1016/S0025-3227(99)00068-7).
- Flanders Marine Institute; Renard Centre of Marine Geology - UGent, 2019. Global contourite distribution database, version 3. Retrieved from: <https://www.marineresources.org>.
- Fronval, T., Jansen, E., 1996. Late Neogene paleoclimates and paleoceanography in the Iceland-Norwegian Sea: evidence from the Iceland and Voering Plateaus. In: Thiede, J., Myhre, A.M., Firth, J.V., Johnson, G.L., Ruddiman, W.F. (Eds.), *Proceeding Ocean Drilling Program, Scientific Results*, Vol. 151, pp. 455–468.
- Fulthorpe, C.S., Carter, R.M., 1991. Continental-shelf progradation by sediment-drift accretion. *Geol. Soc. Am. Bull.* 103 (2), 300–309. [https://doi.org/10.1130/0016-7606\(1991\)103<0300:CSPBSD>2.3.CO;2](https://doi.org/10.1130/0016-7606(1991)103<0300:CSPBSD>2.3.CO;2).
- GEBCO Compilation Group, 2019. The GEBCO 2019 Grid-a continuous terrain model of the global oceans and land. British Oceanographic Data Centre, National Oceanography Centre, NERC, UK. <https://doi.org/10.5285/836f016a-33be-6ddc-e053-6c86abc0788e>.
- Gebhardt, A.C., Geissler, W.H., Matthiessen, J., Jokat, W., 2014. Changes in current patterns in the Fram Strait at the Pliocene/Pleistocene boundary. *Quat. Sci. Rev.* 92, 179–189. <https://doi.org/10.1016/j.quascirev.2013.07.015>.
- Geissler, W.H., Jokat, W., Brekke, H., 2011. The Yermak Plateau in the Arctic Ocean in the light of reflection seismic data-implication for its tectonic and sedimentary evolution. *Geophys. J. Int.* 187 (3), 1334–1362. <https://doi.org/10.1111/j.1365-246X.2011.05197.x>.
- Gilbert, I.M., Pudsey, C.J., Murray, J.W., 1998. A sediment record of cyclic bottom-current variability from the northwest Weddell Sea. *Sediment. Geol.* 115 (1–4), 185–214. [https://doi.org/10.1016/S0037-0738\(97\)00093-6](https://doi.org/10.1016/S0037-0738(97)00093-6).
- Gołdowski, B., Nielsen, S.B., Clausen, O.R., 2012. Patterns of Cenozoic sediment flux from western Scandinavia. *Basin Res.* 24 (4), 377–400. <https://doi.org/10.1111/j.1365-2117.2011.00530.x>.
- Grøsfjeld, K., Dybkiær, K., Eidvin, T., Riis, F., Rasmussen, E.S., Knies, J., 2019. A Miocene age for the Molo Formation, Norwegian Sea shelf off Vestfjorden, based on marine palynology. *Nor. J. Geol.* 99 (3), 1–25. <https://doi.org/10.17850/njg99-3-6>.
- Gruetzner, J., Uenzelmann-Neben, G., Franke, D., 2012. Variations in sediment transport at the central Argentine continental margin during the Cenozoic. *Geochim. Geophys. Geosyst.* 13 (10) <https://doi.org/10.1029/2012GC004266>.
- Hansen, B., Østerhus, S., 2000. North Atlantic–norctic seas exchanges. *Prog. Oceanogr.* 45 (2), 109–208. [https://doi.org/10.1016/S0079-6611\(99\)00052-X](https://doi.org/10.1016/S0079-6611(99)00052-X).
- Helland-Hansen, W., Sømme, T.O., Martinsen, O.J., Lunt, I., Thurmond, J., 2016. Deciphering Earth's natural hourglasses: perspectives on source-to-sink analysis. *J. Sediment. Res.* 86 (9), 1008–1033. <https://doi.org/10.2110/jsr.2016.56>.
- Helmke, J.P., Bauch, H.A., Erlenkeuser, H., 2003. Development of glacial and interglacial conditions in the Nordic seas between 1.5 and 0.35 Ma. *Quat. Sci. Rev.* 22 (15–17), 1717–1728. [https://doi.org/10.1016/S0277-3791\(03\)00126-4](https://doi.org/10.1016/S0277-3791(03)00126-4).
- Henriksen, S., Vorren, T.O., 1996. Late Cenozoic sedimentation and uplift history on the mid-Norwegian continental shelf. *Planet. Planet. Chang.* 12 (1–4), 171–199. [https://doi.org/10.1016/0921-8181\(95\)00019-4](https://doi.org/10.1016/0921-8181(95)00019-4).
- Henriksen, S., Weimer, P., 1996. High-frequency depositional sequences and stratal stacking patterns in lower Pliocene coastal deltas, mid-Norwegian continental shelf. *AAPG Bull.* 80 (12), 1867–1895. <https://doi.org/10.1306/64EDA226-1724-11D7-8645000102C1865D>.
- Hernández-Molina, J., Llave, E., Somoza, L., Fernández-Puga, M.C., Maestro, A., León, R., et al., 2003. Looking for clues to paleoceanographic imprints: a diagnosis of the Gulf of Cadiz contourite depositional systems. *Geology* 31 (1), 19–22. [https://doi.org/10.1130/0091-7613\(2003\)031<0019:LFCTPI>2.0.CO;2](https://doi.org/10.1130/0091-7613(2003)031<0019:LFCTPI>2.0.CO;2).
- Hernández-Molina, F.J., Paterlini, M., Violante, R., Marshall, P., de Isasi, M., Somoza, L., Rebesco, M., 2009. Contourite depositional system on the Argentine Slope: an exceptional record of the influence of Antarctic water masses. *Geology* 37 (6), 507–510. <https://doi.org/10.1130/G25578A.1>.
- Hernández-Molina, F.J., Soto, M., Piola, A.R., Tomasini, J., Preu, B., Thompson, P., et al., 2016. A contourite depositional system along the Uruguayan continental margin: sedimentary, oceanographic and paleoceanographic implications. *Mar. Geol.* 378, 333–349. <https://doi.org/10.1016/j.margeo.2015.10.008>.
- Hernández-Molina, F.J., Larter, R.D., Maldonado, A., 2017. Neogene to Quaternary Stratigraphic Evolution of the Antarctic Peninsula, Pacific Margin offshore of Adelaide Island: transitions from a non-glacial, through glacially-influenced to a fully glacial state. *Glob. Planet. Chang.* 156, 80–111. <https://doi.org/10.1016/j.gloplacha.2017.07.002>.
- Hjelstuen, B.O., Sejrup, H.P., 2021. Latitudinal variability in the Quaternary development of the Eurasian ice sheets—evidence from the marine domain. *Geology* 49 (3), 346–351. <https://doi.org/10.1130/G48106.1>.
- Hjelstuen, B.O., Eldholm, O., Skogseid, J., 1997. Vøring Plateau diapir fields and their structural and depositional settings. *Mar. Geol.* 144 (1–3), 33–57. [https://doi.org/10.1016/S0025-3227\(97\)00085-6](https://doi.org/10.1016/S0025-3227(97)00085-6).
- Hjelstuen, B.O., Eldholm, O., Skogseid, J., 1999. Cenozoic evolution of the northern Vøring margin. *Geol. Soc. Am. Bull.* 111 (12), 1792–1807. [https://doi.org/10.1130/0016-7606\(1999\)111<1792:CEOTNV>2.3.CO;2](https://doi.org/10.1130/0016-7606(1999)111<1792:CEOTNV>2.3.CO;2).
- Hjelstuen, B.O., Sejrup, H.P., Hafliadason, H., Berg, K., Bryn, P., 2004. Neogene and Quaternary depositional environments on the Norwegian continental margin, 62°N–68°N. *Mar. Geol.* 213 (1–4), 257–276. <https://doi.org/10.1016/j.margeo.2004.10.009>.
- Hutchinson, D.K., Coxall, H.K., O'Regan, M., Nilsson, J., Caballero, R., de Boer, A.M., 2019. Arctic closure as a trigger for Atlantic overturning at the Eocene-Oligocene transition. *Nat. Commun.* 10 (1), 1–9. <https://doi.org/10.1038/s41467-019-11828-z>.
- Jakobsson, M., Backman, J., Rudels, B., Nycander, J., Frank, M., Mayer, L., et al., 2007. The early Miocene onset of a ventilated circulation regime in the Arctic Ocean. *Nature* 447 (7147), 986–990. <https://doi.org/10.1038/nature05924>.
- Jakobsson, M., Mayer, L.A., Bringsenparr, C., Castro, C.F., Mohammad, R., Johnson, P., et al., 2020. The international bathymetric chart of the Arctic Ocean version 4.0. *Scientific Data* 7 (1), 1–14. <https://doi.org/10.1038/s41597-020-0520-9>.
- Jansen, E., Sjøholm, J., 1991. Reconstruction of glaciation over the past 6 Myr from ice-borne deposits in the Norwegian Sea. *Nature* 349, 600–603. <https://doi.org/10.1038/349600a0>.
- Japsen, P., Green, P.F., Chalmers, J.A., Bonow, J.M., 2018. Mountains of southernmost Norway: uplifted Miocene peninsulas and re-exposed Mesozoic surfaces. *J. Geol. Soc.* 175 (5), 721–741. <https://doi.org/10.1144/jgs2017-157>.
- Kaminski, M.A., Silye, L., Kender, S., 2009. Miocene deep-water agglutinated foraminifera from the Lomonosov Ridge and the opening of the Fram Strait. *Micropaleontology* 55, 117–135.
- Kim, S., De Santis, L., Hong, J.K., Cottler, D., Petronio, L., Colizza, E., et al., 2018. Seismic stratigraphy of the Central Basin in northwestern Ross Sea slope and rise, Antarctica: clues to the late Cenozoic ice-sheet dynamics and bottom-current activity. *Mar. Geol.* 395, 363–379. <https://doi.org/10.1016/j.margeo.2017.10.013>.
- Kleman, J., Stroeven, A.P., Lundqvist, J., 2008. Patterns of Quaternary ice sheet erosion and deposition in Fennoscandia and a theoretical framework for explanation. *Geomorphology* 97 (1–2), 73–90. <https://doi.org/10.1016/j.geomorph.2007.02.049>.
- Knies, J., Gaina, C., 2008. Middle Miocene ice sheet expansion in the Arctic: views from the Barents Sea. *Geochim. Geophys. Geosyst.* 9 (2) <https://doi.org/10.1029/2007GC001824>.



- Kristoffersen, Y., 1990. On the tectonic evolution and paleoceanographic significance of the Fram Strait gateway. In: Bleil, U., Thiede, J. (Eds.), *Geological History of the Polar Oceans: Arctic Versus Antarctic*. Springer, Dordrecht, pp. 63–76.
- Kuvaas, B., Kristoffersen, Y., 1991. The Cray Fan: a trough-mouth fan on the Weddell Sea continental margin, Antarctica. *Mar. Geol.* 97 (3–4), 345–362. [https://doi.org/10.1016/0025-3227\(91\)90125-N](https://doi.org/10.1016/0025-3227(91)90125-N).
- Laberg, J.S., & Vorren, T.O. (2000). The Trænadjupet Slide, offshore Norway—morphology, evacuation and triggering mechanisms. *Mar. Geol.*, 171 (1–4), 95–114. doi:[https://doi.org/10.1016/S0025-3227\(00\)00112-2](https://doi.org/10.1016/S0025-3227(00)00112-2).
- Laberg, J.S., Vorren, T.O., 2004. Weichselian and Holocene growth of the northern high-latitude Lofoten Contourite Drift on the continental slope of Norway. *Sediment. Geol.* 164 (1–2), 1–17. <https://doi.org/10.1016/j.sedgeo.2003.07.004>.
- Laberg, J.S., Vorren, T.O., Knutsen, S.-M., 1999. The Lofoten contourite drift off Norway. *Mar. Geol.* 159 (1–4), 1–6. [https://doi.org/10.1016/S0025-3227\(98\)00198-4](https://doi.org/10.1016/S0025-3227(98)00198-4).
- Laberg, J.S., Vorren, T.O., Dowdeswell, J.A., Kenyon, N.H., Taylor, J., 2000. The Andøya Slide and the Andøya Canyon, north-eastern Norwegian–Greenland Sea. *Mar. Geol.* 162 (2–4), 259–275. [https://doi.org/10.1016/S0025-3227\(99\)00087-0](https://doi.org/10.1016/S0025-3227(99)00087-0).
- Laberg, J.S., Dahlgren, T., Vorren, T.O., Hafliðason, H., Bryn, P., 2001. Seismic analyses of Cenozoic contourite drift development in the Northern Norwegian Sea. *Mar. Geophys. Res.* 22 (5), 401–416. <https://doi.org/10.1023/A:1016347632294>.
- Laberg, J.S., Vorren, T.O., Knutsen, S.-M., 2002. The Lofoten Drift, Norwegian Sea. In: Stow, D.A.W., Pudsey, C.J., Howe, J.A., Faugeres, J.-C., Viana, A. (Eds.), *Deep-Water Contourite Systems: Modern Drifts and Ancient Series, Seismic and Sedimentary Characteristics*, vol. 22. Geological Society, London, Memoirs, pp. 57–64.
- Laberg, J.S., Stoker, M.S., Dahlgren, K.I.T., de Haas, H., Hafliðason, H., Hjelstuen, B.O., et al., 2005. Cenozoic alongslope processes and sedimentation on the NW European Atlantic margin. *Mar. Pet. Geol.* 22 (9–10), 1069–1088. <https://doi.org/10.1016/j.marpetgeo.2005.01.008>.
- Laberg, J.S., Vorren, T.O., Kenyon, N.H., Ivanov, M., 2006. Frequency and triggering mechanisms of submarine landslides of the North Norwegian continental margin. *Nor. J. Geol.* 86 (3), 155–161.
- Laberg, J.S., Baeten, N.J., Vanneste, M., Forsberg, C.F., Forwick, M., Hafliðason, H., 2016. Sediment failure affecting muddy contourites on the continental slope offshore northern Norway: lessons learned and some outstanding issues. In: Lamarche, G., Mountjoy, J., Bull, S., Hubble, T., Krastel, S., Lane, E., Micallef, A., Moscardelli, L., Mueller, C., Pecher, I., Woelz, S. (Eds.), *Submarine Mass Movements and their Consequences*, Vol. 41. Springer, pp. 281–289.
- Laberg, J.S., Rydningen, T.A., Forwick, M., Husum, K., 2018. Depositional processes on the distal scoresby Trough Mouth fan (ODP site 987): implications for the pleistocene evolution of the scoresby sand sector of the Greenland ice sheet. *Mar. Geol.* 402, 51–59. <https://doi.org/10.1016/j.margeo.2017.11.018>.
- Lasabuda, A., Geissler, W.H., Laberg, J.S., Knutsen, S.M., Rydningen, T.A., Berglar, K., 2018. Late Cenozoic erosion estimates for the northern Barents Sea: Quantifying glacial sediment input to the Arctic Ocean. *Geochim. Geophys. Geosyst.* 19 (12), 4876–4903. <https://doi.org/10.1029/2018GC007882>.
- Lasabuda, A.P.E., Johansen, N.S., Laberg, J.S., Faleide, J.I., Senger, K., Rydningen, T.A., et al., 2021. Cenozoic uplift and erosion on the Norwegian Barents Shelf—a review. *Earth Sci. Rev.* 217, 103609 <https://doi.org/10.1016/j.earscirev.2021.103609>.
- L'Heureux, J.S., Vanneste, M., Rise, L., Brendryen, J., Forsberg, C.F., Nadim, F., et al., 2013. Stability, mobility and failure mechanism for landslides at the upper continental slope off Vesterålen, Norway. *Mar. Geol.* 346, 192–207. <https://doi.org/10.1016/j.margeo.2013.09.009>.
- Lidmar-Bergström, K., Ollier, C.D., Sulebak, J.R., 2000. Landforms and uplift history of southern Norway. *Glob. Planet. Chang.* 24 (3–4), 211–231. [https://doi.org/10.1016/S0921-8181\(00\)00009-6](https://doi.org/10.1016/S0921-8181(00)00009-6).
- Lidmar-Bergström, K., Näslund, J.-O., Ebert, K., Neubeck, T., Bonow, J.M., 2007. Cenozoic landscape development on the passive margin of northern Scandinavia. *Nor. J. Geol.* 87, 181–196.
- Lidmar-Bergström, K., Bonow, J.M., Japsen, P., 2013. Stratigraphic landscape analysis and geomorphological paradigms: Scandinavia as an example of Phanerozoic uplift and subsidence. *Glob. Planet. Chang.* 100, 153–171. <https://doi.org/10.1016/j.gloplacha.2012.10.015>.
- Lien, Ø.F., Hjelstuen, B.O., Zhang, X., Sejrup, H.P., 2022. Late Plio-Pleistocene evolution of the Eurasian Ice Sheets inferred from sediment input along the northeastern Atlantic continental margin. *Quat. Sci. Rev.* 282, 107433 <https://doi.org/10.1016/j.quascirev.2022.107433>.
- Løseth, H., 2021. Comment on ‘A Miocene age for the Molo Formation, Norwegian Sea shelf off Vest-fjorden, based on marine palynology’. *Nor. J. Geol.* 101 <https://doi.org/10.17850/njg101-1-2>.
- Løseth, H., Henriksen, S., 2005. A Middle to Late Miocene compression phase along the Norwegian passive margin. In: Doré, A.G., Vining, B.A. (Eds.), *Petroleum Geology: North-west Europe and Global Perspectives: Proceedings of the 6th Petroleum Geology Conference*, Vol. 6. Geological Society of London, pp. 845–859.
- Løseth, H., Kyrkjebø, R., Hilde, E., Wild, R.J., Bunkholt, H., 2017. 500 m of rapid base level rise along an inner passive margin—Seismic observations from the Pliocene Molo Formation, mid Norway. *Mar. Pet. Geol.* 86, 268–287. <https://doi.org/10.1016/j.marpetgeo.2017.05.039>.
- Lundin, E., Doré, A.G., 2002. Mid-Cenozoic post-breakup deformation in the ‘passive’ margins bordering the Norwegian–Greenland Sea. *Mar. Pet. Geol.* 19 (1), 79–93. [https://doi.org/10.1016/S0264-8172\(01\)00046-0](https://doi.org/10.1016/S0264-8172(01)00046-0).
- Mangerud, J., Gyllencreutz, R., Lohne, Ø., Svendsen, J.I., 2011. Glacial history of Norway. In: Ehlers, J., Gibbard, P.L., Hughes, P.D. (Eds.), *Developments in Quaternary Sciences*, vol. 15. Elsevier, pp. 279–298.
- McCave, I.N., Manighetti, B., Beveridge, N.A.S., 1995. Circulation in the glacial North Atlantic inferred from grain-size measurements. *Nature* 374 (6518), 149–152. <https://doi.org/10.1038/374149a0>.
- Miller, K.G., Browning, J.V., Schmelz, W.J., Kopp, R.E., Mountain, G.S., Wright, J.D., 2020. Cenozoic sea-level and cryospheric evolution from deep-sea geochemical and continental margin records. *Sci. Adv.* 6 (20), eaaz1346. <https://doi.org/10.1126/sciadv.aaz1346>.
- Miramontes, E., Thiéblemont, A., Babonneau, N., Penven, P., Raison, F., Droz, L., et al., 2021. Contourite and mixed turbidite-contourite systems in the Mozambique Channel (SW Indian Ocean): link between geometry, sediment characteristics and modelled bottom currents. *Mar. Geol.* 437, 106502 <https://doi.org/10.1016/j.margeo.2021.106502>.
- Mitchum, R.M., Vail, P.R., Sangree, J.B., 1977. Seismic stratigraphy and global changes of sea level: Part 6. Stratigraphic interpretation of seismic reflection patterns in depositional sequences: Section 2. Application of seismic reflection configuration to stratigraphic interpretation. In: Payton, C. (Ed.), *Seismic Stratigraphy – Applications to Hydrocarbon Exploration*, vol. 26. American Association of Petroleum Geologists Memoir, pp. 117–133.
- Montelli, A., Dowdeswell, J.A., Ottesen, D., Johansen, S.E., 2017. Ice-sheet dynamics through the Quaternary on the mid-Norwegian continental margin inferred from 3D seismic data. *Mar. Pet. Geol.* 80, 228–242. <https://doi.org/10.1016/j.marpetgeo.2016.12.002>.
- Montelli, A., Dowdeswell, J.A., Ottesen, D., Johansen, S.E., 2018. 3D seismic evidence of buried iceberg ploughmarks from the mid-Norwegian continental margin reveals largely persistent North Atlantic Current through the Quaternary. *Mar. Geol.* 399, 66–83. <https://doi.org/10.1016/j.margeo.2017.11.016>.
- Mosher, D.C., Boggild, K., 2021. Impact of bottom currents on deep water sedimentary processes of Canada Basin, Arctic Ocean. *Earth Planet. Sci. Lett.* 569, 117067 <https://doi.org/10.1016/j.epsl.2021.117067>.
- Mosher, D.C., Yanez-Carrizo, G., 2021. The elusive continental rise: insights from residual bathymetry analysis of the Northwest Atlantic margin. *Earth Sci. Rev.* 217, 103608 <https://doi.org/10.1016/j.earscirev.2021.103608>.
- Mosher, D.C., Campbell, D.C., Gardner, J.V., Piper, D.J.W., Chaytor, J.D., Rebesco, M., 2017. The role of deep-water sedimentary processes in shaping a continental margin: the Northwest Atlantic. *Mar. Geol.* 393, 245–259. <https://doi.org/10.1016/j.margeo.2017.08.018>.
- Newton, A.M.W., Huuse, M., 2017. Late Cenozoic environmental changes along the Norwegian margin. *Mar. Geol.* 393, 216–244. <https://doi.org/10.1016/j.margeo.2017.05.004>.
- Newton, A.M.W., Huuse, M., Brocklehurst, S.H., 2018. A persistent Norwegian Atlantic current through the Pleistocene glacials. *Geophys. Res. Lett.* 45 (11), 5599–5608. <https://doi.org/10.1029/2018GL077819>.
- Nielsen, T., De Santis, L., Dahlgren, K.I.T., Kuijpers, A., Laberg, J.S., Nygård, A., et al., 2005. A comparison of the NW European glaciated margin with other glaciated margins. *Mar. Pet. Geol.* 22 (9–10), 1149–1183. <https://doi.org/10.1016/j.marpetgeo.2004.12.007>.
- Nielsen, T.A.P.M., Knutz, P.C., Kuijpers, A., 2008. Seismic expression of contourite depositional systems. In: Rebesco, M., Camerlenghi, A. (Eds.), *Contourites*, vol. 60. Elsevier, Amsterdam, pp. 301–321.
- Nielsen, S.B., Gallagher, K., Leighton, C., Balling, N., Svenningsen, L., Jacobsen, B.H., et al., 2009. The evolution of western Scandinavian topography: a review of Neogene uplift versus the ICE (isostasy–climate–erosion) hypothesis. *J. Geodyn.* 47 (2–3), 72–95. <https://doi.org/10.1016/j.jog.2008.09.001>.
- Nielsen, T., Andersen, C., Knutz, P.C., Kuijpers, A., 2011. The Middle Miocene to Recent Davis Strait Drift Complex: implications for Arctic–Atlantic water exchange. *Geo-Mar. Lett.* 31 (5), 419–426. <https://doi.org/10.1007/s00367-011-0245-z>.
- Nugraha, H.D., Jackson, C.A.-L., Johnson, H.D., Hodgson, D.M., 2020. Lateral variability in strain along the toewall of a mass transport deposit: a case study from the Makassar Strait, offshore Indonesia. *J. Geol. Soc.* 177 (6), 1261–1279. <https://doi.org/10.1144/jgs2020-071>.
- Nyberg, B., Gawthorpe, R.L., Helland-Hansen, W., 2018a. The distribution of rivers to terrestrial sinks: implications for sediment routing systems. *Geomorphology* 316, 1–23. <https://doi.org/10.1016/j.geomorph.2018.05.007>.
- Nyberg, B., Helland-Hansen, W., Gawthorpe, R.L., Sandbakken, P., Eide, C.H., Sømme, T., et al., 2018b. Revisiting morphological relationships of modern source-to-sink segments as a first-order approach to scale ancient sedimentary systems. *Sediment. Geol.* 373, 111–133. <https://doi.org/10.1016/j.sedgeo.2018.06.007>.
- Orvik, K.A., Niiler, P., 2002. Major pathways of Atlantic water in the northern North Atlantic and Nordic Seas toward Arctic. *Geophys. Res. Lett.* 29 (19) <https://doi.org/10.1029/2002GL015002>, 2–1.
- Osmundsen, P.T., Redfield, T.F., 2011. Crustal taper and topography at passive continental margins. *Terra Nova* 23 (6), 349–361. <https://doi.org/10.1111/j.1365-3121.2011.01014.x>.
- Ottesen, D., Rise, L., Knies, J., Olsen, L., Henriksen, S., 2005. The Vestfjorden-Trænadjupet palaeo-ice stream drainage system, mid-Norwegian continental shelf. *Mar. Geol.* 218 (1–4), 175–189. <https://doi.org/10.1016/j.margeo.2005.03.001>.
- Ottesen, D., Rise, L., Andersen, E.S., Bugge, T., Eidvin, T., 2009. Geological evolution of the Norwegian continental shelf between 61°N and 68°N during the last 3 million years. *Nor. J. Geol.* 89 (4), 251–265.
- Ottesen, D., Batchelor, C.L., Bjarnadóttir, L.R., Wiberg, D.H., Dowdeswell, J.A., 2022. Glacial landforms reveal dynamic ice-sheet behaviour along the mid-Norwegian margin during the last glacial-deglacial cycle. *Quat. Sci. Rev.* 285, 107462 <https://doi.org/10.1016/j.quascirev.2022.107462>.
- Patton, H., Hubbard, A., Heyman, J., Alexandropoulou, N., Lasabuda, A.P.E., Stroeven, A.P., et al., 2022. The extreme yet transient nature of glacial erosion. *Nat. Commun.* 13 (1), 1–14. <https://doi.org/10.1038/s41467-022-35072-0>.
- Pedersen, V.K., Huisman, R.S., Moucha, R., 2016. Isostatic and dynamic support of high topography on a North Atlantic passive margin. *Earth Planet. Sci. Lett.* 446, 1–9. <https://doi.org/10.1016/j.epsl.2016.04.019>.

- Pedersen, V.K., Braun, J., Huismans, R.S., 2018. Eocene to mid-Pliocene landscape evolution in Scandinavia inferred from offshore sediment volumes and pre-glacial topography using inverse modelling. *Geomorphology* 303, 467–485. <https://doi.org/10.1016/j.geomorph.2017.11.025>.
- Piper, D.J.W., 2005. Late Cenozoic evolution of the continental margin of eastern Canada. *Nor. J. Geol.* 85 (4), 305–318.
- Piper, D.J.W., Deptuck, M.E., Mosher, D.C., Hughes Clarke, J.E., Migeon, S., 2012. Erosional and depositional features of glacial meltwater discharges on the eastern Canadian continental margin. In: Prather, B.E., Deptuck, M.E., Mohrig, D., Hoon, B. V., Wynn, R.B. (Eds.), *Application of the Principles of Seismic Geomorphology to Continental-Slope and Base-of-Slope Systems: Case Studies from Seafloor and Near-Seafloor Analogues*, vol. 99. SEPM Special Publication, Tulsa, Oklahoma, pp. 61–80.
- Preu, B., Spieß, V., Schwenk, T., Schneider, R., 2011. Evidence for current-controlled sedimentation along the southern Mozambique continental margin since Early Miocene times. *Geo-Mar. Lett.* 31 (5), 427–435. <https://doi.org/10.1007/s00367-011-0238-y>.
- Rasmussen, T.L., Van Weering, T.C.E., Labeyrie, L., 1997. Climatic instability, ice sheets and ocean dynamics at high northern latitudes during the last glacial period (58–10 KA BP). *Quat. Sci. Rev.* 16 (1), 71–80. [https://doi.org/10.1016/S0277-3791\(96\)00045-5](https://doi.org/10.1016/S0277-3791(96)00045-5).
- Rasmussen, S., Lykke-Andersen, H., Kuijpers, A., Troelstra, S.R., 2003a. Post-Miocene sedimentation at the continental rise of Southeast Greenland: the interplay between turbidity and contour currents. *Mar. Geol.* 196 (1–2), 37–52. [https://doi.org/10.1016/S0025-3227\(03\)00043-4](https://doi.org/10.1016/S0025-3227(03)00043-4).
- Rasmussen, T.L., Thomsen, E., Troelstra, S.R., Kuijpers, A., Prins, M.A., 2003b. Millennial-scale glacial variability versus Holocene stability: changes in planktic and benthic foraminifera faunas and ocean circulation in the North Atlantic during the last 60 000 years. *Mar. Micropaleontol.* 47 (1–2), 143–176. [https://doi.org/10.1016/S0377-8398\(02\)00115-9](https://doi.org/10.1016/S0377-8398(02)00115-9).
- Rasmussen, T.L., Thomsen, E., Nielsen, T., 2014. Water mass exchange between the Nordic seas and the Arctic Ocean on millennial timescale during MIS 4–MIS 2. *Geochem. Geophys. Geosyst.* 15 (3), 530–544. <https://doi.org/10.1002/2013GC005020>.
- Rebesco, M., Stow, D., 2001. Seismic expression of contourites and related deposits: a preface. *Mar. Geophys. Res.* 22 (5), 303–308. <https://doi.org/10.1023/A:1016316913639>.
- Rebesco, M., Larter, R.D., Barker, P.F., Camerlenghi, A., Vanneste, L.E., 1997. The history of sedimentation on the continental rise west of the Antarctic Peninsula. In: Barker, P.F., Cooper, A.K. (Eds.), *Geology and Seismic Stratigraphy of the Antarctic Margin*, 2, Vol. 71, pp. 29–49.
- Rebesco, M., Hernández-Molina, F.J., Van Rooij, D., Wählin, A., 2014. Contourites and associated sediments controlled by deep-water circulation processes: State-of-the-art and future considerations. *Mar. Geol.* 352, 111–154. <https://doi.org/10.1016/j.margeo.2014.03.011>.
- Riis, F., 1996. Quantification of Cenozoic vertical movements of Scandinavia by correlation of morphological surfaces with offshore data. *Glob. Planet. Chang.* 12 (1–4), 331–357. [https://doi.org/10.1016/0921-8181\(95\)00027-5](https://doi.org/10.1016/0921-8181(95)00027-5).
- Riis, F., Fjeldskaar, W., 1992. On the magnitude of the late Tertiary and Quaternary erosion and its significance for the uplift of Scandinavia and the Barents Sea. In: Larsen, R.M., Brekke, H., Larsen, B.T., Talleraas, E. (Eds.), *Structural and Tectonic Modelling and its Application to Petroleum Geology*. Elsevier, pp. 163–185.
- Rise, L., Ottesen, D., Berg, K., Lundin, E., 2005. Large-scale development of the mid-Norwegian margin during the last 3 million years. *Mar. Pet. Geol.* 22 (1–2), 33–44. <https://doi.org/10.1016/j.marpetgeo.2004.10.010>.
- Rise, L., Ottesen, D., Longva, O., Solheim, A., Andersen, E.S., Ayers, S., 2006. The Sklinnaadjupe slide and its relation to the Elsterian glaciation on the mid-Norwegian margin. *Mar. Pet. Geol.* 23 (5), 569–583. <https://doi.org/10.1016/j.marpetgeo.2006.05.005>.
- Rise, L., Chand, S., Hjelstuen, B.O., Hafliadson, H., Bøe, R., 2010. Late Cenozoic geological development of the south Vøring margin, mid-Norway. *Mar. Pet. Geol.* 27 (9), 1789–1803. <https://doi.org/10.1016/j.marpetgeo.2010.09.001>.
- Rise, L., Bøe, R., Riis, F., Bellec, V.K., Laberg, J.S., Eidvin, T., et al., 2013. The Lofoten-Vesterålen continental margin, North Norway: canyons and mass-movement activity. *Mar. Pet. Geol.* 45, 134–149. <https://doi.org/10.1016/j.marpetgeo.2013.04.021>.
- Rodrigues, S., Hernández-Molina, F.J., Kirby, A., 2021. A late cretaceous mixed (turbidite-contourite) system along the Argentine Margin: Paleooceanographic and conceptual implications. *Mar. Pet. Geol.* 123, 104768. <https://doi.org/10.1016/j.marpetgeo.2020.104768>.
- Rokoengen, K., Rise, L., Bryn, P., Frengstad, B., Gustavsen, B., Nygaard, E., Sættem, J., 1995. Upper Cenozoic stratigraphy on the mid-Norwegian continental shelf. *Nor. Geol. Tidsskr.* 75 (2–3), 88–104.
- Rydningen, T.A., Vorren, T.O., Laberg, J.S., Kolstad, V., 2013. The marine-based NW Fennoscandian ice sheet: glacial and deglacial dynamics as reconstructed from submarine landforms. *Quat. Sci. Rev.* 68, 126–141. <https://doi.org/10.1016/j.quascirev.2013.02.013>.
- Rydningen, T.A., Laberg, J.S., Kolstad, V., 2015. Seabed morphology and sedimentary processes on high-gradient trough mouth fans offshore Troms, northern Norway. *Geomorphology* 246, 205–219. <https://doi.org/10.1016/j.geomorph.2015.06.007>.
- Rydningen, T.A., Laberg, J.S., Kolstad, V., 2016. Late Cenozoic evolution of high-gradient trough mouth fans and canyons on the glaciated continental margin offshore Troms, northern Norway—Paleoclimatic implications and sediment yield. *Bulletin* 128 (3–4), 576–596. <https://doi.org/10.1130/B31302.1>.
- Rydningen, T.A., Hogseth, G., Lasabuda, A.P.E., Laberg, J.S., Safronova, P., Forwick, M., 2020. An early Neogene—Early Quaternary contourite drift system on the SW Barents Sea continental margin, Norwegian Arctic. *Geochem. Geophys. Geosyst.* 21 (11). <https://doi.org/10.1029/2020GC009142> e2020GC009142.
- Safronova, P.A., Laberg, J.S., Andreassen, K., Shlykova, V., Vorren, T.O., Chernikov, S., 2017. Late Pliocene—early Pleistocene deep-sea basin sedimentation at high-latitudes: mega-scale submarine slides of the north-western Barents Sea margin prior to the shelf-edge glaciations. *Basin Res.* 29, 537–555. <https://doi.org/10.1111/bre.12161>.
- Smith, A.G., Pickering, K.T., 2003. Oceanic gateways as a critical factor to initiate icehouse Earth. *J. Geol. Soc.* 160 (3), 337–340. <https://doi.org/10.1144/0016-764902-115>.
- Sømme, T.O., Helland-Hansen, W., Martinsen, O.J., Thurmond, J.B., 2009. Relationships between morphological and sedimentological parameters in source-to-sink systems: a basis for predicting semi-quantitative characteristics in subsurface systems. *Basin Res.* 21 (4), 361–387. <https://doi.org/10.1111/j.1365-2117.2009.00397.x>.
- Stephenson, R., Schiffer, C., Peace, A., Nielsen, S.B., Jess, S., 2020. Late Cretaceous–Cenozoic basin inversion and palaeostress fields in the North Atlantic–western Alpine–Tethys realm: implications for intraplate tectonics. *Earth Sci. Rev.* 210, 103252. <https://doi.org/10.1016/j.earscirev.2020.103252>.
- Stoker, M.S., Hoult, R.J., Nielsen, T., Hjelstuen, B.O., Laberg, J.S., Shannon, P.M., et al., 2005. Sedimentary and oceanographic responses to early Neogene compression on the NW European margin. *Mar. Pet. Geol.* 22 (9–10), 1031–1044. <https://doi.org/10.1016/j.marpetgeo.2005.01.009>.
- Stow, D., Smillie, Z., 2020. Distinguishing between deep-water sediment facies: turbidites, contourites and hemipelagites. *Geosciences* 10 (2), 68. <https://doi.org/10.3390/geosciences10020068>.
- Stuevold, L.M., Eldholm, O., 1996. Cenozoic uplift of Fennoscandia inferred from a study of the mid-Norwegian margin. *Glob. Planet. Chang.* 12 (1–4), 359–386. [https://doi.org/10.1016/0921-8181\(95\)00028-3](https://doi.org/10.1016/0921-8181(95)00028-3).
- Talwani, M., Eldholm, O., 1972. Continental margin off Norway: a geophysical study. *Geol. Soc. Am. Bull.* 83 (12), 3575–3606. [https://doi.org/10.1130/0016-7606\(1972\)83\[3575:CMONAG\]2.0.CO;2](https://doi.org/10.1130/0016-7606(1972)83[3575:CMONAG]2.0.CO;2).
- Talwani, M., Eldholm, O., 1977. Evolution of the Norwegian–Greenland Sea. *Geol. Soc. Am. Bull.* 88 (7), 969–999. [https://doi.org/10.1130/0016-7606\(1977\)88<969:EOTNS>2.0.CO;2](https://doi.org/10.1130/0016-7606(1977)88<969:EOTNS>2.0.CO;2).
- Thiede, J., Winkler, A., Wolf-Welling, T., Eldholm, O., Myhre, A.M., Baumann, K.-H., et al., 1998. Late Cenozoic history of the Polar North Atlantic: results from ocean drilling. *Quat. Sci. Rev.* 17 (1–3), 185–208. [https://doi.org/10.1016/S0277-3791\(97\)00076-0](https://doi.org/10.1016/S0277-3791(97)00076-0).
- Tripsanas, E.K., Piper, D.J., Jenner, K.A., Bryant, W.R., 2008. Submarine mass-transport facies: new perspectives on flow processes from cores on the eastern North American margin. *Sedimentology* 55 (1), 97–136. <https://doi.org/10.1111/j.1365-3091.2007.00894.x>.
- Viana, A.R., Almeida, W., Nunes, M.C.V., Bulhões, E.M., 2007. The economic importance of contourites. In: Viana, A.R., Rebesco, M. (Eds.), *Economic and Palaeoceanographic Significance of Contourite Deposits*, vol. 276. Geological Society London, pp. 1–23.
- Vogt, P.R., 1972. The Faeroe—Iceland—Greenland aseismic ridge and the western boundary undercurrent. *Nature* 239 (5367), 79–81. <https://doi.org/10.1038/239079a0>.
- Vorren, T.O., Laberg, J.S., 1997. Trough mouth fans—palaeoclimate and ice-sheet monitors. *Quat. Sci. Rev.* 16 (8), 865–881. [https://doi.org/10.1016/S0277-3791\(97\)00003-6](https://doi.org/10.1016/S0277-3791(97)00003-6).
- Vorren, T.O., Plassen, L., 2002. Deglaciation and palaeoclimate of the Andfjord-Vågsfjord area, North Norway. *Boreas* 31 (2), 97–125. <https://doi.org/10.1111/j.1502-3885.2002.tb01060.x>.
- Vorren, T.O., Laberg, J.S., Blaume, F., Dowdeswell, J.A., Kenyon, N.H., Mienert, J., et al., 1998. The Norwegian–Greenland Sea continental margins: morphology and late Quaternary sedimentary processes and environment. *Quat. Sci. Rev.* 17 (1–3), 273–302. [https://doi.org/10.1016/S0277-3791\(97\)00072-3](https://doi.org/10.1016/S0277-3791(97)00072-3).
- Vorren, T.O., Rydningen, T.A., Baeten, N.J., Laberg, J.S., 2015. Chronology and extent of the Lofoten–Vesterålen sector of the Scandinavian Ice Sheet from 26 to 16 cal. ka BP. *Boreas* 44 (3), 445–458. <https://doi.org/10.1111/bor.12118>.
- Weigelt, E., Jokat, W., Eisermann, H., 2020. Deposition History and Paleo-Current Activity on the Southeastern Lomonosov Ridge and its Eurasian Flank Based on Seismic Data. *Geochem. Geophys. Geosyst.* 21 (11). <https://doi.org/10.1029/2020GC009133> e2020GC009133.
- Wold, C.N., 1994. Cenozoic sediment accumulation on drifts in the northern North Atlantic. *Paleoceanography* 9 (6), 917–941. <https://doi.org/10.1029/94PA01438>.
- Wright, J.D., 1998. The role of the Greenland–Scotland ridge in Neogene climate changes. In: Crowley, T.J., Burke, K.C. (Eds.), *Tectonic Boundary Conditions for Climate Reconstruction*, vol. 39. Oxford University Press, Oxford, UK, pp. 192–211.
- Wu, N., Jackson, C.A.L., Johnson, H.D., Hodgson, D.M., Nugraha, H.D., 2020. Mass-transport complexes (MTCs) document subsidence patterns in a northern Gulf of Mexico salt minibasin. *Basin Res.* 32 (6), 1300–1327. <https://doi.org/10.1111/bre.12429>.
- Zachos, J., Pagani, M., Sloan, L., Thomas, E., Billups, K., 2001. Trends, rhythms, and aberrations in global climate 65 Ma to present. *Science* 292 (5517), 686–693. <https://doi.org/10.1126/science.1059412>.